Nonlinear dynamics of coupled transverse-rotational waves in granular chains

Qicheng Zhang[1,2,3,*], Olga Umnova[4] and Rodolfo Venegas[5]
[1]*Acoustic Science and Technology Laboratory, Harbin Engineering University, Harbin 150001, China*
[2]*Key Laboratory of Marine Information Acquisition and Security (Harbin Engineering University), Ministry of Industry and Information Technology, Harbin 150001, China*
[3]*College of Underwater Acoustic Engineering, Harbin Engineering University, Harbin 150001, China*
e-mail address: zhangqicheng@hrbeu.edu.cn
[4]*Acoustic Research Centre, University of Salford, Salford M5 4WT, United Kingdom*
[5]*University Austral of Chile, Institute of Acoustics, P.O. Box 567, Valdivia, Chile*

The nonlinear dynamics of coupled waves in one-dimensional granular chains with and without a substrate is theoretically studied accounting for quadratic nonlinearity. The multiple time scale method is used to derive the nonlinear dispersion relations for infinite granular chains and to obtain the wave solutions for semi-infinite systems. It is shown that the sum-frequency and difference-frequency components of the coupled transverse-rotational waves are generated due to their nonlinear interactions with the longitudinal wave. Nonlinear resonances are not present in the chain with no substrate where these frequency components have low amplitudes and exhibit beating oscillations. In the chain positioned on a substrate two types of nonlinear resonances are predicted. At resonance, the fundamental frequency wave amplitudes decrease and the generated frequency component amplitudes increase along the chain, accompanied by the oscillations due to the wave numbers asynchronism. The results confirm the possibility of a highly efficient energy transfer between the waves of different frequencies, which could find applications in the design of acoustic devices for energy transfer and energy rectification.

Keywords: Transverse-rotational waves, Nonlinear dynamics, Granular crystals, Energy transfer
PACS: 45.70.-n, 43.25.+y, 63.20.Pw

I. INTRODUCTION

Granular crystals, usually composed of spherical particles interacting via nonlinear contacts [**1**], have attracted much attention in the last few decades due to their complex linear and nonlinear wave dynamics [**2**]. Typically, the nonlinear contacts can be tuned by changing the external compressions, which permit the systems to behave in near-linear, weakly nonlinear, and strongly nonlinear regimes.

In the near-linear regime, the granular crystals behave as one type of periodic phononic structures, exhibiting wave dispersion, band gaps, and localized modes. This offers the systems a flexible way of designing acousto-elastic filters [**3**,**4**], protectors [**5**,**6**] and lenses [**7**]. Furthermore, the granular crystals have been shown to possess interparticle shear interactions and rotations leading to complex wave dynamics whose associated wave dispersion can be tuned [**8**,**9**] and that exhibits phenomena such as zero group velocity modes and accidental degeneracy [**10**,**11**].

In the nonlinear regimes, the wave process and energy transfer in the granular crystals is of interest for practical applications. For example, the efficient energy transfer might be useful in various engineering applications, such as acoustic energy rectifiers and switchers [**12**,**13**], energy harvesting devices [**14**,**15**], and targeted energy converters [**16**]. Common examples that have been extensively studied in weakly nonlinear granular crystals are the second harmonic (SH) generation and related energy transmission. These have been evidenced in various configurations including the monoatomic granular chain [**17**], the diatomic chain [**18**], the linear-nonlinear coupled chains [**19**], and the square-packed granular waveguide [**20**]. The amplitudes of the fundamental frequency (FF) wave and the SH are characterized by the spatial beating oscillations, resulting from the wave dispersion, both in nonlinear monoatomic and diatomic granular chains [**17**,**18**]. Moreover, the nonlinear resonances were demonstrated in a Fermi-Pasta-Ulam (FPU) diatomic chain [**21**] and in the linear-nonlinear coupled chains [**19**]. The time-space (or equivalently frequency-wave number) synchronism condition at the resonance results in a continuous amplification of the generated SH amplitude and a continuous attenuation of the FF wave amplitude along the chain. Theoretically, this could result in a complete energy transfer between the two wave components. Alternatively, the energy transfer can be achieved by nonlinear bifurcations, arising from the defect localized modes [**12**] and finite size of weakly nonlinear granular systems [**13**]. Different from that of the SH generations, the redistributed energy based on bifurcations can be more efficient and can be transferred to a lower frequency range, e.g., to the subharmonics.

For the strongly nonlinear granular crystals, the highly efficient energy transfer can be achieved [**22**] when the undesirable mechanical energy is transferred and dissipated

from a primary oscillation chain to another nonlinear coupled chain [**16**,**23**,**24**] or a nonlinear end attachment [**25**].

Most of the studies on wave dynamics of nonlinear granular crystals considers only a single type of wave motion, namely the longitudinal wave, for which the SH generations are induced by its self-action (or sometimes called self-interaction) nonlinearity effects. Considering transverse and the rotational degrees of freedom (DOFs) in the weakly nonlinear chain enables different types of interactions and hence is of interest for the fundamental understanding of the wave dynamics. For example, the work by Wallen and Boechler [**26**] studied the shear to longitudinal mode conversion in a compressed 2D array of particles arranged in a hexagonal lattice, accounting for translational and rotational DOFs. Such conversion is achieved via longitudinal nonlinear self-action-based SH generation for cases where the FF wave is purely longitudinal or transverse–rotational.

This present work investigates the coupled transverse-rotational (TR) wave dynamics in a one-dimensional (1D) weakly nonlinear granular chain without and with a substrate where it is placed on and interact with, by taking into account, simultaneously, three DOFs, i.e., coupled longitudinal, transverse and rotational waves. We focus on the nonlinear wave components with combined frequencies, i.e., the sum-frequency (SF) and the difference-frequency (DF), which are generated due to nonlinear interactions between the longitudinal and the TR waves. The chain dynamics is described by three coupled equations of motions (EOMs) with quadratic nonlinearity accounted for. The multiple time scale method (MTSM) [**27**-**30**] is used to solve the nonlinear EOMs in order to approximate the nonlinear dispersion curves for the infinite granular chains as well as for investigating the nonlinear wave solutions for the semi-infinite systems where the boundary conditions are formulated.

II. MODEL

We consider two configurations of the granular chains in this paper. The configuration 1 is the monoatomic granular chain of spherical particles in contact, as illustrated by Fig. 1(a). The particles have a mass *m*, moment of inertia *I*, radius *R*, Young's modulus *E,* shear modulus *G*, and Poisson's ratio *v*. The chain is pre-compressed by a static force *P* exerted along the horizontal direction. Three DOFs for each particle are considered to investigate the dynamics of the system. These are the longitudinal displacement u_j, transverse displacement w_j, and rotation $\varphi_j = R\theta_j$, where θ_j is the angle of rotation. The contact between the particles is characterized by the normalized normal stiffness coefficients k_1 and k_2, as well as the normalized shear stiffness coefficients s_1 and s_2. Note that k_2 and s_2 are the coefficients that characterize the quadratic nonlinearity considered in this work. An additional coupling between the chain and a substrate is accounted for in the configuration 2, where the pre-compression force F is exerted along the vertical direction, as shown in Fig. 1(b). The chain-substrate coupling is characterized by the normalized linear normal stiffness coefficient g_n and the shear stiffness coefficients g_s. As discussed in Ref. [**11**], an additional tangential force Q is applied along the horizontal direction between the chain and the substrate to tune their couplings by means of setting the shear stiffness coefficient value. The exact expressions for all these coefficients are given in Sec. II.B.

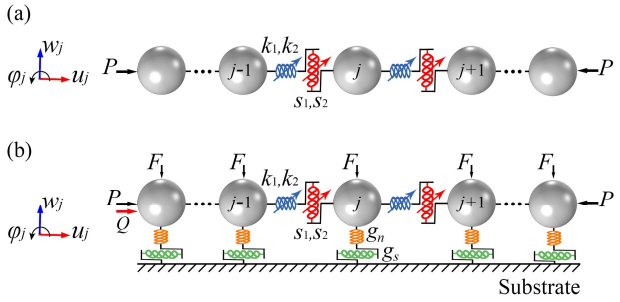

FIG. 1. (Color online) Diagram of the granular chains with three degrees of freedom. (a) Monoatomic granular chain without a substrate. (b) Monoatomic granular chain on a substrate.

A. Contact models

The normal and shear contacts between two particles are described by the Hertz and Hertz-Mindlin models [**1**], respectively. The relationships between the forces and relative longitudinal and transverse displacements Δu and Δw are given by

$$f_N = -A\left[\delta_0 - \Delta u\right]^{\frac{3}{2}}, \tag{1a}$$

$$f_S = B\Delta w\left[\delta_0 - \Delta u\right]^{\frac{1}{2}}, \tag{1b}$$

where $A = (4/3)E_{eff}R_{eff}^{1/2}$ and $B = 8G_{eff}R_{eff}^{1/2}$ are the stiffness coefficients that depend on the geometrical and material properties. $E_{eff} = E/2\left(1-\nu^2\right)$, $G_{eff} = G/2(2-\nu)$ and $R_{eff} = R/2$ are the effective Young's modulus, effective shear modulus and the effective radius. $\delta_0 = \left(P/A\right)^{2/3}$ is the static overlap length induced by the pre-compression *P*. Note that in Eqs. (1) the contact is assumed to be tensionless, which means that the terms in brackets vanish if they become negative.

In the weakly nonlinear regime ($\Delta u < \delta_0$), the functions of displacements (1) can be expanded in Taylor series up to the quadratic terms as

$$f_N = -A\delta_0^{\frac{3}{2}} + \frac{3}{2}A\delta_0^{\frac{1}{2}} \cdot \Delta u - \frac{3}{8}A\delta_0^{-\frac{1}{2}} \cdot \Delta u^2, \qquad (2a)$$

$$f_S = B\delta_0^{\frac{1}{2}} \cdot \Delta w - \frac{1}{2}B\delta_0^{-\frac{1}{2}} \cdot \Delta w \Delta u. \qquad (2b)$$

The contact between the particle and the substrate are governed by the same models described above, but with the adjusted parameters E_{eff1}, G_{eff1}, R_{eff1}, δ_1, where δ_1 is the static overlap length of the particle-substrate contact induced by the pre-compression F. In the particular case where the particles and substrate are composed of the same materials, these parameters are

$$E_{eff1} = E_{eff}, G_{eff1} = G_{eff}, R_{eff1} = 2R_{eff}, \delta_1 = \left[F \Big/ \left(\sqrt{2}A\right)\right]^{\frac{2}{3}}. \qquad (3)$$

In order to induce a linear coupling between the chain and the substrate, a vertical pre-compression force that is larger than the horizontal pre-compression force, is applied so that the static overlap lengths satisfy $\delta_1 \gg \delta_0$. Then, the forces between a particle and the substrate can be considered approximately in the linear limit as

$$t_N = \frac{3\sqrt{2}}{2}A\delta_1^{\frac{1}{2}} \cdot w, \qquad (4a)$$

$$t_S = \sqrt{2}B\delta_1^{\frac{1}{2}}\left(1 - \frac{Q}{\kappa F}\right)^{\frac{1}{3}} \cdot u. \qquad (4b)$$

Here Eq. (4b) defines the shear force-displacement relationship that is tunable by the additional tangential loading Q, as provided by Eq. (15) in Ref. [**11**], and κ is the static friction coefficient between the chain and the substrate [see Fig. 1(b)].

B. Nonlinear equations of motion

The wave dynamics in granular chains is modelled by the nonlinear EOMs for each particle. Without loss of generality, the EOMs of the j-th particle in the chain-substrate system are

$$m\frac{\partial^2 u_j}{\partial t^2} = A\left[\delta_0 - \left(u_j - u_{j-1}\right)\right]^{\frac{3}{2}} - A\left[\delta_0 - \left(u_{j+1} - u_j\right)\right]^{\frac{3}{2}} - \sqrt{2}B\delta_1^{\frac{1}{2}}\left(1 - \frac{Q}{\kappa F}\right)^{\frac{1}{3}}\left(u_j - R\theta_j\right), \qquad (5a)$$

$$m\frac{\partial^2 w_j}{\partial t^2} = -B\left[w_j - w_{j-1} - R\left(\theta_j + \theta_{j-1}\right)\right]\left[\delta_0 - \left(u_j - u_{j-1}\right)\right]^{\frac{1}{2}} + B\left[w_{j+1} - w_j - R\left(\theta_{j+1} + \theta_j\right)\right]\left[\delta_0 - \left(u_{j+1} - u_j\right)\right]^{\frac{1}{2}} - \frac{3\sqrt{2}}{2}A\delta_1^{\frac{1}{2}}w_j, \qquad (5b)$$

$$I\frac{\partial^2 \theta_j}{\partial t^2} = -BR\left[R\left(\theta_j + \theta_{j-1}\right) - \left(w_j - w_{j-1}\right)\right]\left[\delta_0 - \left(u_j - u_{j-1}\right)\right]^{\frac{1}{2}} - BR\left[R\left(\theta_{j+1} + \theta_j\right) - \left(w_{j+1} - w_j\right)\right]\left[\delta_0 - \left(u_{j+1} - u_j\right)\right]^{\frac{1}{2}} + \sqrt{2}B\delta_1^{\frac{1}{2}}\left(1 - \frac{Q}{\kappa F}\right)^{\frac{1}{3}}\left(u_j - R\theta_j\right). \qquad (5c)$$

We introduce the following dimensionless spatial and temporal variables (retaining the same symbols, u_j, w_j, φ_j and t for them)

$$u_j = \frac{u_j}{D_0}, w_j = \frac{w_j}{D_0}, \varphi_j = \frac{R\theta_j}{D_0}, t = \omega_0 t, \qquad (6)$$

where D_0 is a characteristic amplitude and $\omega_0 = \sqrt{3A\delta_0^{1/2}/2m}$ is the characteristic angular frequency. Note that in an externally driven system, the characteristic amplitude D_0 can be considered as the amplitude of the harmonic displacement imposed on the boundary particle. We also define a small parameter $\varepsilon = D_0/\delta_0$ which describes the strength of the nonlinearity of the system.

By Inserting the normalized variables into the EOMs, and using expansions for the contact forces in Eqs. (2), we obtain

$$\frac{\partial^2 u_j}{\partial t^2} = k_1\left(u_{j-1} + u_{j+1} - 2u_j\right) - g_s\left(u_j - \varphi_j\right) + \varepsilon k_2\left[\left(u_j - u_{j-1}\right)^2 - \left(u_{j+1} - u_j\right)^2\right], \qquad (7a)$$

$$\frac{\partial^2 w_j}{\partial t^2} = s_1\left(w_{j-1} + w_{j+1} - 2w_j\right) + s_1\left(\varphi_{j-1} - \varphi_{j+1}\right) - g_n w_j + \varepsilon s_2\begin{bmatrix}\left(w_j - w_{j-1} - \left(\varphi_j + \varphi_{j-1}\right)\right)\left(u_j - u_{j-1}\right) \\ -\left(w_{j+1} - w_j - \left(\varphi_{j+1} + \varphi_j\right)\right)\left(u_{j+1} - u_j\right)\end{bmatrix}, \qquad (7b)$$

$$\frac{\partial^2 \varphi_j}{\partial t^2} = -r_1\left(\varphi_{j-1} + \varphi_{j+1} + 2\varphi_j\right) + r_1\left(w_{j+1} - w_{j-1}\right) + g_r\left(u_j - \varphi_j\right) + \varepsilon r_2\begin{bmatrix}\left(\varphi_j + \varphi_{j-1} - \left(w_j - w_{j-1}\right)\right)\left(u_j - u_{j-1}\right) \\ +\left(\varphi_{j+1} + \varphi_j - \left(w_{j+1} - w_j\right)\right)\left(u_{j+1} - u_j\right)\end{bmatrix}. \qquad (7c)$$

In Eqs. (7), the normalized linear and quadratic nonlinear stiffness coefficients between the particles are

$$k_1 = 1, k_2 = \frac{1}{4}, s_1 = \frac{2}{3}\frac{B}{A}, s_2 = \frac{1}{3}\frac{B}{A}, r_1 = \frac{s_1}{I'}, r_2 = \frac{s_2}{I'}, \quad (8)$$

and the normalized linear stiffness coefficients that characterize the coupling between the particles and the substrate are

$$g_n = \sqrt{2}\left(\frac{\delta_1}{\delta_0}\right)^{\frac{1}{2}}, g_s = \frac{2\sqrt{2}B}{3A}\left(\frac{\delta_1}{\delta_0}\right)^{\frac{1}{2}}\left(1-\frac{Q}{\kappa F}\right)^{\frac{1}{3}}, g_r = \frac{g_s}{I'}, \quad (9)$$

where $I' = I/mR^2 = 0.4$ is the normalized moment of inertia of the homogeneous spherical particles. It is worth noting that the bending rigidities are neglected for all the contacts considered in this work since their magnitudes can be proven to be much smaller than that of the normal and shear stiffness [31].

In Secs. III.A-III.B, the Eqs. (7) will be reduced to those that describe the dynamics of the monoatomic chain without a substrate [Fig. 1(a)] by setting $g_n = 0$ and $g_s = 0$. Then, in Sec. III.D, the nonlinear resonances will be considered for the chain on a substrate [Fig. 1(b)] by assuming that only the linear normal coupling g_n exists between the chain and the substrate, that is, $g_n \neq 0$, $g_s = 0$. In particular, the shear stiffness coefficient $g_s = 0$ can be practically achieved, for example, by setting the additional tangential loading $Q = \kappa F$ between the chain and the substrate, as can be seen from Eqs. (9). In both cases, one can note that the longitudinal wave is decoupled from the transverse and rotational waves, and its nonlinearity is induced by the terms u_j^2, i.e., the self-action takes place (see e.g., Ref. [**18**] and [**19**]). However, the transverse and the rotational waves are coupled. They are denoted as TR (transverse-rotational) waves, and their nonlinearities are attributed to the interactions with the longitudinal wave (i.e., the $u_j w_j$ and $u_j \varphi_j$ terms).

III. THEORY

A. Multiple time scale analysis

To investigate the effect of nonlinearity on the wave dynamics, we use the MTSM to solve the nonlinear EOMs of the monoatomic granular chain with no substrate. The procedure for determining the wave dynamics in the chain-substrate system can be performed in much the same way. In MTSM, the small nonlinearity parameter ε is treated as a perturbation and the displacements (or rotation) can be asymptotically expanded in power series with terms quadratic in ε retained. For example,

$$u_j(\tau_0, \tau_1, \tau_2) = u_j^{(0)}(\tau_0, \tau_1, \tau_2) + \varepsilon u_j^{(1)}(\tau_0, \tau_1, \tau_2) + \varepsilon^2 u_j^{(2)}(\tau_0, \tau_1, \tau_2), \quad (10)$$

where $\tau_0 = t$, $\tau_1 = \varepsilon\tau_0$ and $\tau_2 = \varepsilon^2\tau_0$ represent different time scales. The derivatives of the displacement with respect to time are then

$$\frac{\partial u_j}{\partial t} = \frac{\partial u_j^{(0)}}{\partial \tau_0} + \varepsilon\left(\frac{\partial u_j^{(1)}}{\partial \tau_0} + \frac{\partial u_j^{(0)}}{\partial \tau_1}\right) + \varepsilon^2\left(\frac{\partial u_j^{(2)}}{\partial \tau_0} + \frac{\partial u_j^{(1)}}{\partial \tau_1} + \frac{\partial u_j^{(0)}}{\partial \tau_2}\right), \quad (11a)$$

$$\frac{\partial^2 u_j}{\partial t^2} = \frac{\partial^2 u_j^{(0)}}{\partial \tau_0^2} + \varepsilon\left(\frac{\partial^2 u_j^{(1)}}{\partial \tau_0^2} + 2\frac{\partial^2 u_j^{(0)}}{\partial \tau_1 \partial \tau_0}\right) + \varepsilon^2\left(\frac{\partial^2 u_j^{(2)}}{\partial \tau_0^2} + 2\frac{\partial^2 u_j^{(1)}}{\partial \tau_1 \partial \tau_0} + 2\frac{\partial^2 u_j^{(0)}}{\partial \tau_2 \partial \tau_0} + \frac{\partial^2 u_j^{(0)}}{\partial \tau_1^2}\right). \quad (11b)$$

Similar expansions can be written for w_j and φ_j and their derivatives.

Under these conditions, the nonlinear EOMs are decomposed into three groups of equations in powers of ε, namely the zeroth, first and second order EOMs, respectively. At each order, we provide the nonlinear dispersion relation correctors for an infinite granular chain and the solutions for different wave components for a semi-infinite system for which the boundary conditions are formulated.

1. Zeroth order EOMs

The zeroth order (or linear) EOMs are

$$\frac{\partial^2 u_j^{(0)}}{\partial \tau_0^2} + k_1\left(2u_j^{(0)} - u_{j-1}^{(0)} - u_{j+1}^{(0)}\right) = 0, \quad (12a)$$

$$\frac{\partial^2 w_j^{(0)}}{\partial \tau_0^2} + s_1\left(2w_j^{(0)} - w_{j-1}^{(0)} - w_{j+1}^{(0)}\right) + s_1\left(\varphi_{j+1}^{(0)} - \varphi_{j-1}^{(0)}\right) = 0, \quad (12b)$$

$$\frac{\partial^2 \varphi_j^{(0)}}{\partial \tau_0^2} + r_1\left(2\varphi_j^{(0)} + \varphi_{j-1}^{(0)} + \varphi_{j+1}^{(0)}\right) + r_1\left(w_{j-1}^{(0)} - w_{j+1}^{(0)}\right) = 0. \quad (12c)$$

The general solutions for the fundamental frequency (FF) waves are looked for in the following form

$$u_j^{(0)} = A_0(\tau_1, \tau_2)e^{i\alpha_{jL}} + c.c., \quad (13a)$$

$$w_j^{(0)} = B_0(\tau_1, \tau_2)e^{i\alpha_{jTR}} + c.c., \quad (13b)$$

$$\varphi_j^{(0)} = C_0(\tau_1, \tau_2)e^{i\alpha_{jTR}} + c.c.. \quad (13c)$$

In Eqs. (13), $\alpha_{jL} = \mu(\omega_{L0})j - \omega_{L0}\tau_0$ and $\alpha_{jTR} = \mu(\omega_{TR0})j - \omega_{TR0}\tau_0$ represent the phase terms of the FF waves, where

ω is the angular frequency normalized by ω_0, and μ is the corresponding wave number normalized by the lattice constant $a = 2R$. The acronym *c.c.* stands for the "complex conjugates" of the preceding terms. Furthermore,

$$A_0(\tau_1,\tau_2) = \left|A_0(\tau_1,\tau_2)\right| e^{-i(\omega_{L1}\tau_1+\omega_{L2}\tau_2)}, \quad (14a)$$

$$B_0(\tau_1,\tau_2) = \left|B_0(\tau_1,\tau_2)\right| e^{-i(\omega_{TR1}\tau_1+\omega_{TR2}\tau_2)}, \quad (14b)$$

$$C_0(\tau_1,\tau_2) = \left|C_0(\tau_1,\tau_2)\right| e^{-i(\omega_{TR1}\tau_1+\omega_{TR2}\tau_2)}, \quad (14c)$$

where $\left|A_0(\tau_1,\tau_2)\right|$, $\left|B_0(\tau_1,\tau_2)\right|$ and $\left|C_0(\tau_1,\tau_2)\right|$ are the displacement and rotation amplitudes that permit slow time evolution, and ω_{TR1} (or ω_{L1}) and ω_{TR2} (or ω_{L2}) are the nonlinear frequency correctors to the linear dispersion relations. These will be determined by solving the higher order EOMs.

Substituting Eqs. (13) into Eqs. (12) and keeping only the linear terms yields an eigenvalue problem

$$\begin{pmatrix} 2k_1\left(1-\cos\left[\mu(\omega_{L0})\right]\right)-\omega_{L0}^2 & 0 & 0 \\ 0 & 2s_1\left(1-\cos\left[\mu(\omega_{TR0})\right]\right)-\omega_{TR0}^2 & 2is_1\sin\left[\mu(\omega_{TR0})\right] \\ 0 & -2ir_1\sin\left[\mu(\omega_{TR0})\right] & 2r_1\left(1+\cos\left[\mu(\omega_{TR0})\right]\right)-\omega_{TR0}^2 \end{pmatrix} \begin{pmatrix} |A_0| \\ |B_0| \\ |C_0| \end{pmatrix} = 0, \quad (15)$$

which results in the linear dispersion relations for the longitudinal and TR waves

$$\omega_{L0} = \sqrt{2k_1\left(1-\cos\left[\mu(\omega_{L0})\right]\right)}, \quad (16a)$$

$$\omega_{TR0}^{+} = \sqrt{2r_1\left(1+\cos\left[\mu(\omega_{TR0})\right]\right)+2s_1\left(1-\cos\left[\mu(\omega_{TR0})\right]\right)}, \quad (16b)$$

$$\omega_{TR0}^{-} = 0, \quad (16c)$$

where ω_{TR0}^{+} is the higher frequency mode of the TR waves, and ω_{TR0}^{-} is the lower frequency mode. The latter is a zero-frequency mode, i.e., the non-propagative mode with zero group velocity, resulting from the counterbalance between the transverse and the rotational motions in the monoatomic chain [**9**,**31**], and it will not be considered in the analysis below. In addition, the ratio of the transverse and rotational wave amplitudes for each mode can be found from Eq. (15) and reads as

$$\frac{|C_0|}{|B_0|} = \left|\frac{2s_1\left(1-\cos\left[\mu(\omega_{TR0})\right]\right)-\omega_{TR0}^2}{-2is_1\sin\left[\mu(\omega_{TR0})\right]}\right|. \quad (17)$$

2. First order EOMs

The first order EOMs in ε are

$$\frac{\partial^2 u_j^{(1)}}{\partial\tau_0^2} + k_1\left(2u_j^{(1)} - u_{j-1}^{(1)} - u_{j+1}^{(1)}\right) = -2\frac{\partial^2 u_j^{(0)}}{\partial\tau_1\partial\tau_0} + k_2\left[\left(u_j^{(0)} - u_{j-1}^{(0)}\right)^2 - \left(u_{j+1}^{(0)} - u_j^{(0)}\right)^2\right], \quad (18a)$$

$$\frac{\partial^2 w_j^{(1)}}{\partial\tau_0^2} + s_1\left(2w_j^{(1)} - w_{j-1}^{(1)} - w_{j+1}^{(1)}\right) + s_1\left(\varphi_{j+1}^{(1)} - \varphi_{j-1}^{(1)}\right) = -2\frac{\partial^2 w_j^{(0)}}{\partial\tau_1\partial\tau_0} + s_2\begin{bmatrix}\left(w_j^{(0)} - w_{j-1}^{(0)} - \left(\varphi_j^{(0)} + \varphi_{j-1}^{(0)}\right)\right)\left(u_j^{(0)} - u_{j-1}^{(0)}\right) \\ -\left(w_{j+1}^{(0)} - w_j^{(0)} - \left(\varphi_{j+1}^{(0)} + \varphi_j^{(0)}\right)\right)\left(u_{j+1}^{(0)} - u_j^{(0)}\right)\end{bmatrix}, \quad (18b)$$

$$\frac{\partial^2 \varphi_j^{(1)}}{\partial\tau_0^2} + r_1\left(2\varphi_j^{(1)} + \varphi_{j-1}^{(1)} + \varphi_{j+1}^{(1)}\right) + r_1\left(w_{j-1}^{(1)} - w_{j+1}^{(1)}\right) = -2\frac{\partial^2 \varphi_j^{(0)}}{\partial\tau_1\partial\tau_0} + r_2\begin{bmatrix}\left(\varphi_j^{(0)} + \varphi_{j-1}^{(0)} - \left(w_j^{(0)} - w_{j-1}^{(0)}\right)\right)\left(u_j^{(0)} - u_{j-1}^{(0)}\right) \\ +\left(\varphi_{j+1}^{(0)} + \varphi_j^{(0)} - \left(w_{j+1}^{(0)} - w_j^{(0)}\right)\right)\left(u_{j+1}^{(0)} - u_j^{(0)}\right)\end{bmatrix}. \quad (18c)$$

Substituting the zeroth order solutions (13) into Eqs. (18) results in the following equations

$$\frac{\partial^2 u_j^{(1)}}{\partial\tau_0^2} + k_1\left(2u_j^{(1)} - u_{j-1}^{(1)} - u_{j+1}^{(1)}\right) = 2i\omega_{L0}\frac{\partial A_0}{\partial\tau_1}e^{i\alpha_{jL}} + a_1 e^{i2\alpha_{jL}} + c.c., \quad (19a)$$

$$\frac{\partial^2 w_j^{(1)}}{\partial\tau_0^2} + s_1\left(2w_j^{(1)} - w_{j-1}^{(1)} - w_{j+1}^{(1)}\right) + s_1\left(\varphi_{j+1}^{(1)} - \varphi_{j-1}^{(1)}\right) = 2i\omega_{TR0}\frac{\partial B_0}{\partial\tau_1}e^{i\alpha_{jTR}} + b_1 e^{i\left(\alpha_{jTR}+\alpha_{jL}\right)} + d_1 e^{i\left(\alpha_{jTR}-\alpha_{jL}\right)} + c.c., \quad (19b)$$

$$\frac{\partial^2 \varphi_j^{(1)}}{\partial \tau_0^2} + r_1\left(2\varphi_j^{(1)} + \varphi_{j-1}^{(1)} + \varphi_{j+1}^{(1)}\right) + r_1\left(w_{j-1}^{(1)} - w_{j+1}^{(1)}\right)$$
$$= 2i\omega_{TR0}\frac{\partial C_0}{\partial \tau_1}e^{i\alpha_{jTR}} + c_1 e^{i\left(\alpha_{jTR}+\alpha_{jL}\right)} + e_1 e^{i\left(\alpha_{jTR}-\alpha_{jL}\right)} + c.c.. \quad (19c)$$

One can note from the right-hand sides of Eqs. (19) that, apart from the FF waves (i.e., the $e^{i\alpha_{jTR}}$ terms), the combined frequency components of the TR waves, that is, the sum-frequency (SF) component (i.e., the $e^{i(\alpha_{jTR}+\alpha_{jL})}$ terms) and the difference-frequency (DF) component (i.e., the $e^{i(\alpha_{jTR}-\alpha_{jL})}$ terms), are generated by the nonlinear wave interactions.

By eliminating the secular terms [**30**], which are those proportional to $e^{i\alpha_{jL}}$ and $e^{i\alpha_{jTR}}$ in Eqs. (19), we come to the conclusion that the quantities A_0 , B_0 and C_0 are independent of τ_1 . As a consequence, the first order frequency correctors to the linear dispersion relations given by Eqs. (14) vanish.

Meanwhile, by equating the wave component terms in Eqs. (19), the first order wave solutions are obtained as the superposition of the particular (subscript *P*) solutions and general solutions of the homogeneous (subscript *H*) equations, i.e.,

$$u_j^{(1)} = u_{j,P}^{(1)} + u_{j,H}^{(1)}$$
$$= A_{1P}(\tau_2)e^{i2\alpha_{jL}} + A_{1H}(\tau_2)e^{i2\beta_{jL}} + c.c., \quad (20a)$$

$$w_j^{(1)} = w_{j,P}^{(1)} + w_{j,H}^{(1)}$$
$$= B_{1P}(\tau_2)e^{i\left(\alpha_{jTR}+\alpha_{jL}\right)} + D_{1P}(\tau_2)e^{i\left(\alpha_{jTR}-\alpha_{jL}\right)}$$
$$+B_{1H}(\tau_2)e^{i\left(\beta_{jTR}+\beta_{jL}\right)} + D_{1H}(\tau_2)e^{i\left(\beta_{jTR}-\beta_{jL}\right)} + c.c., \quad (20b)$$

$$\varphi_j^{(1)} = \varphi_{j,P}^{(1)} + \varphi_{j,H}^{(1)}$$
$$= C_{1P}(\tau_2)e^{i\left(\alpha_{jTR}+\alpha_{jL}\right)} + E_{1P}(\tau_2)e^{i\left(\alpha_{jTR}-\alpha_{jL}\right)}$$
$$+C_{1H}(\tau_2)e^{i\left(\beta_{jTR}+\beta_{jL}\right)} + E_{1H}(\tau_2)e^{i\left(\beta_{jTR}-\beta_{jL}\right)} + c.c., \quad (20c)$$

where $2\alpha_{jL} = 2\mu(\omega_{L0})j - 2\omega_{L0}\tau_0$ and $2\beta_{jL} = \mu(2\omega_{L0})j - 2\omega_{L0}\tau_0$ are two phase terms of the second harmonic (SH) of the longitudinal wave, and

$$\alpha_{jTR} \pm \alpha_{jL} = \left[\mu(\omega_{TR0}) \pm \mu(\omega_{L0})\right]j - \left(\omega_{TR0} \pm \omega_{L0}\right)\tau_0, \quad (21a)$$

$$\beta_{jTR} \pm \beta_{jL} = \mu\left(\omega_{TR0} \pm \omega_{L0}\right)j - \left(\omega_{TR0} \pm \omega_{L0}\right)\tau_0, \quad (21b)$$

are the phases of the SF component (plus sign) and DF component (minus sign) of the TR waves.

The coefficients of the particular solutions in Eqs. (20) are given by

$$A_{1P} = a_1 \cdot \Phi_0\left(2\omega_{L0}, 2\mu(\omega_{L0})\right), \quad (22a)$$

$$B_{1P} = b_1 \cdot \Phi_1\left(\omega_{TR0} + \omega_{L0}, \mu(\omega_{TR0}) + \mu(\omega_{L0})\right)$$
$$+ c_1 \cdot \Phi_2\left(\omega_{TR0} + \omega_{L0}, \mu(\omega_{TR0}) + \mu(\omega_{L0})\right), \quad (22b)$$

$$D_{1P} = d_1 \cdot \Phi_1\left(\omega_{TR0} - \omega_{L0}, \mu(\omega_{TR0}) - \mu(\omega_{L0})\right)$$
$$+ e_1 \cdot \Phi_2\left(\omega_{TR0} - \omega_{L0}, \mu(\omega_{TR0}) - \mu(\omega_{L0})\right), \quad (22c)$$

$$C_{1P} = b_1 \cdot \Phi_3\left(\omega_{TR0} + \omega_{L0}, \mu(\omega_{TR0}) + \mu(\omega_{L0})\right)$$
$$+ c_1 \cdot \Phi_4\left(\omega_{TR0} + \omega_{L0}, \mu(\omega_{TR0}) + \mu(\omega_{L0})\right), \quad (22d)$$

$$E_{1P} = d_1 \cdot \Phi_3\left(\omega_{TR0} - \omega_{L0}, \mu(\omega_{TR0}) - \mu(\omega_{L0})\right)$$
$$+ e_1 \cdot \Phi_4\left(\omega_{TR0} - \omega_{L0}, \mu(\omega_{TR0}) - \mu(\omega_{L0})\right). \quad (22e)$$

The pre-factors a_1, b_1, c_1, d_1 and e_1 are given in the Appendix A and the Φ functions read as

$$\Phi_0(\omega,\mu) = \frac{1}{2k_1(1-\cos\mu) - \omega^2}, \quad (23a)$$

$$\Phi_1(\omega,\mu) = \frac{2r_1(1+\cos\mu) - \omega^2}{\Phi_{Den}(\omega,\mu)}, \quad (23b)$$

$$\Phi_2(\omega,\mu) = \frac{-2s_1\sin\mu}{\Phi_{Den}(\omega,\mu)}, \quad (23c)$$

$$\Phi_3(\omega,\mu) = \frac{2r_1\sin\mu}{\Phi_{Den}(\omega,\mu)}, \quad (23d)$$

$$\Phi_4(\omega,\mu) = \frac{2s_1(1-\cos\mu) - \omega^2}{\Phi_{Den}(\omega,\mu)}, \quad (23e)$$

with

$$\Phi_{Den}(\omega,\mu) = \left[2s_1(1-\cos\mu) - \omega^2\right]\left[2r_1(1+\cos\mu) - \omega^2\right]$$
$$- 4s_1 r_1 \sin^2\mu. \quad (23f)$$

To determine the coefficients of the general solutions of the homogeneous equations in Eqs. (20), the boundary conditions [$u_0^{(1)}(2\omega_{L0}) = 0$, $w_0^{(1)}(\omega_{TR0} \pm \omega_{L0}) = 0$ and $\varphi_0^{(1)}(\omega_{TR0} \pm \omega_{L0}) = 0$] for a semi-infinite chain are formulated. These correspond to the absence of the SH and combined frequency components at the boundary, named as the $j = 0$ particle. One therefore has that

$$A_{1H} = -A_{1P}, \quad (24a)$$

$$B_{1H} = -B_{1P}, D_{1H} = -D_{1P}, \quad (24b)$$

$$C_{1H} = -C_{1P}, E_{1H} = -E_{1P}. \quad (24c)$$

Under these conditions, the first order solutions (20) are simplified to

$$u_j^{(1)} = 2i\sin\left(\frac{\Delta\mu_L}{2}j\right)e^{i\frac{\Delta\mu_L}{2}j}A_{1P}\cdot e^{i2\beta_{jL}} + c.c., \tag{25a}$$

$$w_j^{(1)} = 2i\sin\left(\frac{\Delta\mu_{TR}^{+}}{2}j\right)e^{i\frac{\Delta\mu_{TR}^{+}}{2}j}B_{1P}\cdot e^{i\left(\beta_{jTR}+\beta_{jL}\right)} + 2i\sin\left(\frac{\Delta\mu_{TR}^{-}}{2}j\right)e^{i\frac{\Delta\mu_{TR}^{-}}{2}j}D_{1P}\cdot e^{i\left(\beta_{jTR}-\beta_{jL}\right)} + c.c., \tag{25b}$$

$$\varphi_j^{(1)} = 2i\sin\left(\frac{\Delta\mu_{TR}^{+}}{2}j\right)e^{i\frac{\Delta\mu_{TR}^{+}}{2}j}C_{1P}\cdot e^{i\left(\beta_{jTR}+\beta_{jL}\right)} + 2i\sin\left(\frac{\Delta\mu_{TR}^{-}}{2}j\right)e^{i\frac{\Delta\mu_{TR}^{-}}{2}j}E_{1P}\cdot e^{i\left(\beta_{jTR}-\beta_{jL}\right)} + c.c., \tag{25c}$$

where the expressions for the wave number mismatch due to the wave dispersion are

$$\Delta\mu_L = 2\mu(\omega_{L0}) - \mu(2\omega_{L0}), \tag{26a}$$

$$\Delta\mu_{TR}^{+} = \left[\mu(\omega_{TR0}) + \mu(\omega_{L0})\right] - \mu(\omega_{TR0}+\omega_{L0}), \tag{26b}$$

$$\Delta\mu_{TR}^{-} = \left[\mu(\omega_{TR0}) - \mu(\omega_{L0})\right] - \mu(\omega_{TR0}-\omega_{L0}). \tag{26c}$$

3. Second order EOMs

According to the previous results, the second order EOMs need to be considered to calculate the frequency correctors to the dispersion relations. They are

$$\frac{\partial^2 u_j^{(2)}}{\partial\tau_0^2} + k_1\left(2u_j^{(2)} - u_{j-1}^{(2)} - u_{j+1}^{(2)}\right) = -2\frac{\partial^2 u_j^{(1)}}{\partial\tau_1\partial\tau_0} - 2\frac{\partial^2 u_j^{(0)}}{\partial\tau_2\partial\tau_0} - \frac{\partial^2 u_j^{(0)}}{\partial\tau_1^2} + 2k_2\begin{bmatrix}\left(u_j^{(0)} - u_{j-1}^{(0)}\right)\left(u_j^{(1)} - u_{j-1}^{(1)}\right) \\ -\left(u_{j+1}^{(0)} - u_j^{(0)}\right)\left(u_{j+1}^{(1)} - u_j^{(1)}\right)\end{bmatrix}, \tag{27a}$$

$$\frac{\partial^2 w_j^{(2)}}{\partial\tau_0^2} + s_1\left(2w_j^{(2)} - w_{j-1}^{(2)} - w_{j+1}^{(2)}\right) + s_1\left(\varphi_{j+1}^{(2)} - \varphi_{j-1}^{(2)}\right) = -2\frac{\partial^2 w_j^{(1)}}{\partial\tau_1\partial\tau_0} - 2\frac{\partial^2 w_j^{(0)}}{\partial\tau_2\partial\tau_0} - \frac{\partial^2 w_j^{(0)}}{\partial\tau_1^2} + s_2\begin{bmatrix}\left(w_j^{(0)} - w_{j-1}^{(0)} - \left(\varphi_j^{(0)} + \varphi_{j-1}^{(0)}\right)\right)\left(u_j^{(1)} - u_{j-1}^{(1)}\right) \\ -\left(w_{j+1}^{(0)} - w_j^{(0)} - \left(\varphi_{j+1}^{(0)} + \varphi_j^{(0)}\right)\right)\left(u_{j+1}^{(1)} - u_j^{(1)}\right)\end{bmatrix} + s_2\begin{bmatrix}\left(w_j^{(1)} - w_{j-1}^{(1)} - \left(\varphi_j^{(1)} + \varphi_{j-1}^{(1)}\right)\right)\left(u_j^{(0)} - u_{j-1}^{(0)}\right) \\ -\left(w_{j+1}^{(1)} - w_j^{(1)} - \left(\varphi_{j+1}^{(1)} + \varphi_j^{(1)}\right)\right)\left(u_{j+1}^{(0)} - u_j^{(0)}\right)\end{bmatrix}, \tag{27b}$$

$$\frac{\partial^2 \varphi_j^{(2)}}{\partial\tau_0^2} + r_1\left(2\varphi_j^{(2)} + \varphi_{j-1}^{(2)} + \varphi_{j+1}^{(2)}\right) + r_1\left(w_{j-1}^{(2)} - w_{j+1}^{(2)}\right) = -2\frac{\partial^2 \varphi_j^{(1)}}{\partial\tau_1\partial\tau_0} - 2\frac{\partial^2 \varphi_j^{(0)}}{\partial\tau_2\partial\tau_0} - \frac{\partial^2 \varphi_j^{(0)}}{\partial\tau_1^2} + r_2\begin{bmatrix}\left(\varphi_j^{(0)} + \varphi_{j-1}^{(0)} - \left(w_j^{(0)} - w_{j-1}^{(0)}\right)\right)\left(u_j^{(1)} - u_{j-1}^{(1)}\right) \\ +\left(\varphi_{j+1}^{(0)} + \varphi_j^{(0)} - \left(w_{j+1}^{(0)} - w_j^{(0)}\right)\right)\left(u_{j+1}^{(1)} - u_j^{(1)}\right)\end{bmatrix} + r_2\begin{bmatrix}\left(\varphi_j^{(1)} + \varphi_{j-1}^{(1)} - \left(w_j^{(1)} - w_{j-1}^{(1)}\right)\right)\left(u_j^{(0)} - u_{j-1}^{(0)}\right) \\ +\left(\varphi_{j+1}^{(1)} + \varphi_j^{(1)} - \left(w_{j+1}^{(1)} - w_j^{(1)}\right)\right)\left(u_{j+1}^{(0)} - u_j^{(0)}\right)\end{bmatrix}. \tag{27c}$$

Using the method employed for solving the first order EOMs (see Appendix B), the second order frequency correctors to the linear dispersion relations in Eqs. (14) can be obtained by setting the secular terms to zero, i.e.,

$$\omega_{L2} = \frac{2ik_2\left(2\sin\left[\mu(\omega_{L0})\right] - \sin\left[2\mu(\omega_{L0})\right]\right)\cdot\left|\bar{A}_0\right|A_{1P}}{\omega_{L0}\left|A_0\right|}, \tag{28a}$$

$$\omega_{TR2} = \frac{is_2\left(\sin\left[\mu(\omega_{L0})\right]+\sin\left[\mu(\omega_{TR0})\right]-\sin\left[\mu(\omega_{TR0})+\mu(\omega_{L0})\right]\right)\cdot\left|\bar{A}_0\right|B_{1P}}{\omega_{TR0}\left|B_0\right|}$$
$$+\frac{s_2\left(1-\cos\left[\mu(\omega_{L0})\right]-\cos\left[\mu(\omega_{TR0})\right]+\cos\left[\mu(\omega_{TR0})+\mu(\omega_{L0})\right]\right)\cdot\left|\bar{A}_0\right|C_{1P}}{\omega_{TR0}\left|B_0\right|}$$
$$-\frac{is_2\left(\sin\left[\mu(\omega_{L0})\right]-\sin\left[\mu(\omega_{TR0})\right]+\sin\left[\mu(\omega_{TR0})-\mu(\omega_{L0})\right]\right)\cdot\left|A_0\right|D_{1P}}{\omega_{TR0}\left|B_0\right|}$$
$$+\frac{s_2\left(1-\cos\left[\mu(\omega_{L0})\right]-\cos\left[\mu(\omega_{TR0})\right]+\cos\left[\mu(\omega_{TR0})-\mu(\omega_{L0})\right]\right)\cdot\left|A_0\right|E_{1P}}{\omega_{TR0}\left|B_0\right|}, \tag{28b}$$

$$\omega^*_{TR2} = \frac{r_2\left(1-\cos\left[\mu(\omega_{L0})\right]+\cos\left[\mu(\omega_{TR0})\right]-\cos\left[\mu(\omega_{TR0})+\mu(\omega_{L0})\right]\right)\cdot\left|\bar{A}_0\right|B_{1P}}{\omega_{TR0}\left|C_0\right|}$$
$$+\frac{ir_2\left(\sin\left[\mu(\omega_{L0})\right]-\sin\left[\mu(\omega_{TR0})\right]+\sin\left[\mu(\omega_{TR0})+\mu(\omega_{L0})\right]\right)\cdot\left|\bar{A}_0\right|C_{1P}}{\omega_{TR0}\left|C_0\right|}$$
$$+\frac{r_2\left(1-\cos\left[\mu(\omega_{L0})\right]+\cos\left[\mu(\omega_{TR0})\right]-\cos\left[\mu(\omega_{TR0})-\mu(\omega_{L0})\right]\right)\cdot\left|A_0\right|D_{1P}}{\omega_{TR0}\left|C_0\right|}$$
$$-\frac{ir_2\left(\sin\left[\mu(\omega_{L0})\right]+\sin\left[\mu(\omega_{TR0})\right]-\sin\left[\mu(\omega_{TR0})-\mu(\omega_{L0})\right]\right)\cdot\left|A_0\right|E_{1P}}{\omega_{TR0}\left|C_0\right|}. \tag{28c}$$

The two frequency correctors of the TR wave follow from Eqs. (27b) and (27c), respectively, and $\bar{X}$ represents the complex conjugate of X.

Considering the same boundary conditions as previously, the second order wave solutions, that contain only the contributions of the FF waves, are given by

$$u_j^{(2)} = -2i\sin\left(\frac{\Delta\mu_L}{2}j\right)e^{-i\frac{\Delta\mu_L}{2}j}A_{2P}\cdot e^{i\alpha_{jL}} + c.c., \tag{29a}$$

$$w_j^{(2)} = -2i\sin\left(\frac{\Delta\mu_{TR}^+}{2}j\right)e^{-i\frac{\Delta\mu_{TR}^+}{2}j}B_{2P}\cdot e^{i\alpha_{jTR}}$$
$$-2i\sin\left(\frac{\Delta\mu_{TR}^-}{2}j\right)e^{-i\frac{\Delta\mu_{TR}^-}{2}j}D_{2P}\cdot e^{i\alpha_{jTR}} + c.c., \tag{29b}$$

$$\varphi_j^{(2)} = -2i\sin\left(\frac{\Delta\mu_{TR}^+}{2}j\right)e^{-i\frac{\Delta\mu_{TR}^+}{2}j}C_{2P}\cdot e^{i\alpha_{jTR}}$$
$$-2i\sin\left(\frac{\Delta\mu_{TR}^-}{2}j\right)e^{-i\frac{\Delta\mu_{TR}^-}{2}j}E_{2P}\cdot e^{i\alpha_{jTR}} + c.c.. \tag{29c}$$

The coefficients A_{2P}, B_{2P}, C_{2P}, D_{2P} and E_{2P} can be found in the Appendix B.

B. Nonlinear dispersion relations and wave solutions

So far, the dispersion relation correctors and the wave solutions at each relevant order have been obtained. The dispersion relations including correctors up to the second order in ε are given by

$$\omega_L = \omega_{L0} + \varepsilon^2\omega_{L2}, \tag{30a}$$

$$\omega_{TR} = \omega_{TR0} + \varepsilon^2\left(\omega_{TR2} + \omega^*_{TR2}\right). \tag{30b}$$

By combining the terms for different wave components, the resulting FF wave solutions read as

$$u_{j,FF} = \left[\left|A_0\right| - \varepsilon^2 2i\sin\left(\frac{\Delta\mu_L}{2}j\right)e^{-i\frac{\Delta\mu_L}{2}j}A_{2P}\right]\cdot e^{i\alpha_{jL}} + c.c., \tag{31a}$$

$$w_{j,FF} = \begin{bmatrix}\left|B_0\right| - \varepsilon^2 2i\sin\left(\frac{\Delta\mu_{TR}^+}{2}j\right)e^{-i\frac{\Delta\mu_{TR}^+}{2}j}B_{2P}\\ -\varepsilon^2 2i\sin\left(\frac{\Delta\mu_{TR}^-}{2}j\right)e^{-i\frac{\Delta\mu_{TR}^-}{2}j}D_{2P}\end{bmatrix}\cdot e^{i\alpha_{jTR}} + c.c., \tag{31b}$$

$$\varphi_{j,FF}=\left[\begin{array}{c}\left|C_0\right|-\varepsilon^2 2i\sin\left(\dfrac{\Delta\mu_{TR}^{+}}{2}j\right)e^{-i\frac{\Delta\mu_{TR}^{+}}{2}j}C_{2P}\\ -\varepsilon^2 2i\sin\left(\dfrac{\Delta\mu_{TR}^{-}}{2}j\right)e^{-i\frac{\Delta\mu_{TR}^{-}}{2}j}E_{2P}\end{array}\right]\cdot e^{i\alpha_{jTR}}+c.c..\tag{31c}$$

The SF components of the TR waves (and the SH of the longitudinal wave) are given by

$$u_{j,SH}=\varepsilon 2i\sin\left(\frac{\Delta\mu_L}{2}j\right)e^{i\frac{\Delta\mu_L}{2}j}A_{1P}\cdot e^{i2\beta_{jL}}+c.c.,\tag{32a}$$

$$w_{j,SF}=\varepsilon 2i\sin\left(\frac{\Delta\mu_{TR}^{+}}{2}j\right)e^{i\frac{\Delta\mu_{TR}^{+}}{2}j}B_{1P}\cdot e^{i\left(\beta_{jTR}+\beta_{jL}\right)}+c.c.,\tag{32b}$$

$$\varphi_{j,SF}=\varepsilon 2i\sin\left(\frac{\Delta\mu_{TR}^{+}}{2}j\right)e^{i\frac{\Delta\mu_{TR}^{+}}{2}j}C_{1P}\cdot e^{i\left(\beta_{jTR}+\beta_{jL}\right)}+c.c.,\tag{32c}$$

and the DF components are

$$w_{j,DF}=\varepsilon 2i\sin\left(\frac{\Delta\mu_{TR}^{-}}{2}j\right)e^{i\frac{\Delta\mu_{TR}^{-}}{2}j}D_{1P}\cdot e^{i\left(\beta_{jTR}-\beta_{jL}\right)}+c.c.,\tag{33a}$$

$$\varphi_{j,DF}=\varepsilon 2i\sin\left(\frac{\Delta\mu_{TR}^{-}}{2}j\right)e^{i\frac{\Delta\mu_{TR}^{-}}{2}j}E_{1P}\cdot e^{i\left(\beta_{jTR}-\beta_{jL}\right)}+c.c..\tag{33b}$$

C. Nonlinear beatings

From the solutions given by Eqs. (31-33), it is seen that the amplitudes of the FF wave and the combined frequency components vary periodically with the particle number *j*. This is described as the nonlinear beating phenomenon [**17**,**18**], which results from the wave dispersion, as shown in Eqs. (26).

Similar to the temporal beatings caused by the interference between two acoustic waves of different frequencies, the nonlinear beatings here are spatial and result from the interference between two acoustic waves with different wave numbers. For instance, the two SF components of wave numbers $\mu_1=\mu(\omega_{TR0}+\omega_{L0})$ and $\mu_2=\mu(\omega_{TR0})+\mu(\omega_{L0})$, as presented by Eqs. (20), are out of phase, which leads to the maxima of one wave to cancel the minima of the other. When the two SF components of the wave numbers are in phase, their maxima sum up, which leads to an increase of amplitude. The beating period is proven to be half the difference between the wave numbers of the two original waves, as given by Eqs. (32-33). Accordingly, the SF component amplitudes of the TR waves reach the maximum when $\left|\Delta\mu_{TR}^{+}\right|j=(2n+1)\pi$, or alternatively at the particle $j=(2n+1)\pi\Big/\left|\Delta\mu_{TR}^{+}\right|$, n=0,1,2,…, and the DF component amplitudes maximize at $j=(2n+1)\pi\Big/\left|\Delta\mu_{TR}^{-}\right|$. The oscillation period of the FF wave amplitudes is determined by those of the DF and SF components, i.e., their lowest common multiple.

However, it should be emphasized that the amplitudes of the beating in the solutions (32-33) should be of the order $\mathrm{O}(\varepsilon)$ [or $B_{1P},C_{1P},D_{1P},E_{1P}\approx\mathrm{O}(1)$] in order to comply with the assumptions made in MTSM. In other words, this indicates that our description is valid when a small fraction of injected energy transfers to the combined frequency components due to the weak nonlinearity of the system.

D. Nonlinear resonances

In addition to the nonlinear beatings, the system could exhibit nonlinear resonances at specific wave numbers and frequencies when the Φ functions (23) become singular. This gives the following conditions for the nonlinear resonance to occur

$$\Phi_{Den}\left(\omega_{TR0}+\omega_{L0},\mu(\omega_{TR0})+\mu(\omega_{L0})\right)=0,\tag{34a}$$

$$\text{or }\Phi_{Den}\left(\omega_{TR0}-\omega_{L0},\mu(\omega_{TR0})-\mu(\omega_{L0})\right)=0,\tag{34b}$$

where Φ_{Den} is the denominator of the Φ functions.

The Φ functions have various forms for different configurations of the granular chains, which will determine the existence (or absence) of the nonlinear resonance. For instance, for the monoatomic granular chain without substrate [Fig. 1(a)], the denominator of the Φ functions takes the form in Eq. (23f), which cannot be zero within the first Brillouin zone $\mu\in[-\pi,\pi]$, meaning the absence of a nonlinear resonance.

To identify the nonlinear resonances, we consider configuration 2 [Fig. 1(b)] with only the linear normal coupling g_n existing between the chain and the substrate, that is, $g_n\neq 0$, $g_s=0$. Unlike configuration 1 [dispersion relations given by Eqs. 16(b-c)], two linear TR modes, both with non-zero frequencies, are excited in this case due to the chain-substrate coupling,

$$\omega_{TR0}^{\pm\,2} = \frac{2s_1\left(1-\cos\left[\mu(\omega_{TR0})\right]\right)+2r_1\left(1+\cos\left[\mu(\omega_{TR0})\right]\right)+g_n}{2} \pm \frac{\sqrt{\left(2s_1\left(1-\cos\left[\mu(\omega_{TR0})\right]\right)+2r_1\left(1+\cos\left[\mu(\omega_{TR0})\right]\right)+g_n\right)^2-8r_1\left(1+\cos\left[\mu(\omega_{TR0})\right]\right)g_n}}{2}. \quad (35)$$

The denominator of the Φ functions now becomes

$$\Phi_{Den}(\omega,\mu) = \left[2s_1\left(1-\cos\mu\right)+g_n-\omega^2\right]\left[2r_1\left(1+\cos\mu\right)-\omega^2\right] - 4s_1r_1\sin^2\mu. \quad (36)$$

This equation shows that there could exist zero points that correspond to the resonance phenomenon due to the additional tunable coefficient g_n. The nonlinear resonance conditions (34) could be satisfied and after some algebraic steps, one can find the relationships between the wave numbers at the resonance

$$\mu(\omega_{TR}+\omega_L) = 2n\pi - \left[\mu(\omega_{TR})+\mu(\omega_L)\right], \quad (37a)$$

$$\text{or } \mu(\omega_{TR}-\omega_L) = 2n\pi - \left[\mu(\omega_{TR})-\mu(\omega_L)\right], \quad (37b)$$

where n=0,1,2,…, denotes the Bloch periodicity of the wave number. Similar resonance condition between the FF wave and SH, but with the time-space synchronism condition $\mu(2\omega)=2\mu(\omega)$ (the wave number mismatch $\Delta\mu=0$), can be found in nonlinear FPU lattices [**21**]. With the conditions (37) for combination resonances, however, it could be achieved even for the case $\Delta\mu\neq 0$ [see Eqs. (26)]. This phenomenon is referred to as the resonances with asynchronism condition and is one of the key contributions of this paper. In particular, the condition (37a) describes a nonlinear resonance occurring between the FF and SF components, while the condition (37b) corresponds to the resonance occurring between the FF and DF components.

We will show numerically in Sec. IV that, unlike the weak energy transfer carried by the amplitude beatings, at the nonlinear resonance the energy could, in theory, be transferred completely from the FF component to the SF or DF components in non-dissipative system.

IV. RESULTS AND DISCUSSION

In this section we discuss the nonlinear dispersion relations and the dynamics of different wave components in the granular chains. To verify the theoretical analysis in Sec. III, numerical simulations are carried out by integrating the nonlinear EOMs (7) with the 4th-order Runge-Kutta scheme (ODE113) implemented in the commercial software MATLAB [**32**].

The longitudinal and TR waves are generated by applying harmonic excitations to a boundary before the first particle of a semi-infinite chain as $u_0 = |A_0|\cos(\omega_L t)$, $w_0 = |B_0|\cos(\omega_{TR}t)$ and $\varphi_0 = |C_0|\sin(\omega_{TR}t)$, where $|A_0|$, $|B_0|$ and $|C_0|$ are the amplitudes normalized by $\varepsilon\delta_0$ (as described in Sec. II), and the ratio of $|B_0|$ and $|C_0|$ is approximated by Eq. (17) using the linear dispersion relations. To simulate only the forward waves propagating in the semi-infinite chain, appropriate simulation time and chain length are chosen so that the reflected waves do not reach the particle sites to be considered in the analysis.

The particles and the substrate are assumed to be made of the neodymium magnet material (NdFeB N35) in this work. In practical implementation of the system, the use of magnet material could provide controllable pre-compressions between the neighboring particles and between the particles and the substrate. The material and geometrical parameters are: density $\rho = 7500\,\text{kg/m}^3$, Young's modulus $E = 160\text{GPa}$, Poisson's ratio $\nu = 0.3$, (estimated) static friction coefficient $\kappa = 0.1$, and sphere radius $R = 7.5\text{mm}$. The pre-compression force exerted along the horizontal direction is $P = 30\text{N}$, while that exerted along the vertical direction is chosen to a larger value, i.e., $F = 85\text{N}$, such that the particle-substrate contact can be considered linear. The additional tangential force between the chain and substrate is hence chosen to $Q = \kappa F = 8.5\text{N}$ to set the shear stiffness coefficient g_s to zero, as discussed in Sec. II. It is worth mentioning that all the considered contacts under these pre-compressions are within the Hertz model limitations [**1**], i.e., the contact radii are much smaller than the static overlap lengths. Under these conditions, the normalized stiffness coefficients, described in Sec. II, are given by

$$k_1 = 1, s_1 = 0.79, r_1 = 1.98,$$
$$k_2 = 0.25, s_2 = 0.40, r_2 = 0.98,$$
$$g_n = 2, g_s = 0, g_r = 0. \quad (38)$$

The small nonlinearity parameter is chosen as $\varepsilon = 0.1$ in order to keep the system operating in the weakly nonlinear regime.

A. Nonlinear wave dynamics in a granular chain without substrate

As predicted by Eqs. (28), the nonlinear dispersion relations of the TR waves are not independent of the frequency of the longitudinal wave ω_L. To ensure that both

the SF and DF components of the TR waves belong to the propagating modes, the normalized frequency of the longitudinal wave is first fixed at a small value of $\omega_L = 0.3$.

The nonlinear dispersion curves within the first Brillouin zone of the monoatomic chain without substrate are plotted in Fig. 2. The solid lines with a positive group velocity represent the dispersion curves for the waves propagating in the forward direction, while the dotted lines correspond to those for the backward waves [**33**]. To conduct the analysis of the forward wave dynamics in a semi-infinite chain, the dispersion relations for the backward waves will not be plotted in what follows.

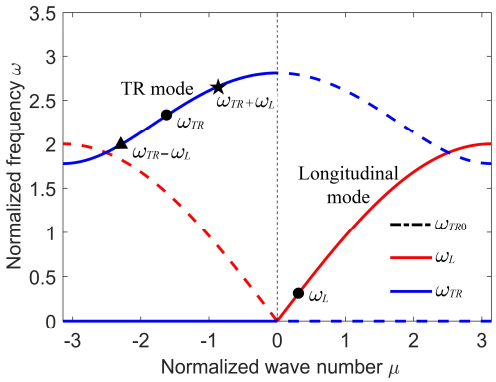

FIG. 2. (Color online) Nonlinear dispersion relations of the monoatomic granular chain with no substrate. The solid lines denote the dispersion curves for the forward waves, whereas the dotted lines correspond to those for the backward waves. Circle markers: fundamental frequency (FF) waves; star marker: sum-frequency (SF) component; triangle marker: difference-frequency (DF) component.

One can observe that the weak quadratic nonlinearity ($\varepsilon = 0.1$) considered in this work leads to a small correction to the linear TR wave dispersion relations (black dashed lines that are almost entirely covered by the nonlinear dispersion curves). Moreover, no resonance effect is observed. This is because, in this case, the Φ functions (23) do not exhibit the singularity that is the signature of the nonlinear resonance.

Now we investigate the nonlinear wave dynamics of different wave components of the TR mode, as those illustrated in Fig. 2. Their frequencies and corresponding wave numbers are listed in Table I. The normalized amplitudes of the incident waves in all the following discussion are $|A_0| = 1$, $|B_0| = 1$ but $|C_0|$ is set by the amplitude ratio in Eq. (17) for different configurations.

TABLE I. Parameters of the wave components on the propagating TR mode

Component	Longitudinal FF wave	TR FF wave	TR SF component	TR DF component
Frequency	$\omega_L = 0.3$	$\omega_{TR} = 2.3$	$\omega_{TR} + \omega_L = 2.6$	$\omega_{TR} - \omega_L = 2.0$
Wave number	$\mu(\omega_L) = 0.299$	$\mu(\omega_{TR}) = -1.669$	$\mu(\omega_{TR} + \omega_L) = -1.015$	$\mu(\omega_{TR} - \omega_L) = -2.272$
Location	Longitudinal mode	TR mode	TR mode	TR mode

The nonlinear dynamics of the longitudinal wave in the monoatomic chain is the same as in Ref. [**17**]. Hence this is not described here. The amplitude profiles of the FF wave, SF and DF components of the rotational wave along the first 100 particles are shown in Fig. 3 (a), (b) and (c), respectively. As it follows from Eqs. (31-33), those of the transverse wave behave similarly and they are not presented for the sake of brevity. It is clear that the numerical results (blue dots) agree well with the theoretical predictions (red lines).

As predicted by Eqs. (32-33), the amplitudes of the generated wave components exhibit oscillations with increasing particle position j. For instance, the maximum amplitudes of the SF component appear at $j \approx 9, 27, 45, \ldots$, while those of the DF component at $j \approx 11, 33, 55, \ldots$. The amplitude of the FF wave oscillates with fractions of the energy transferred to the SF and DF components. However, most of the energy still concentrates in oscillations with the FF due to the weak nonlinearity of the system.

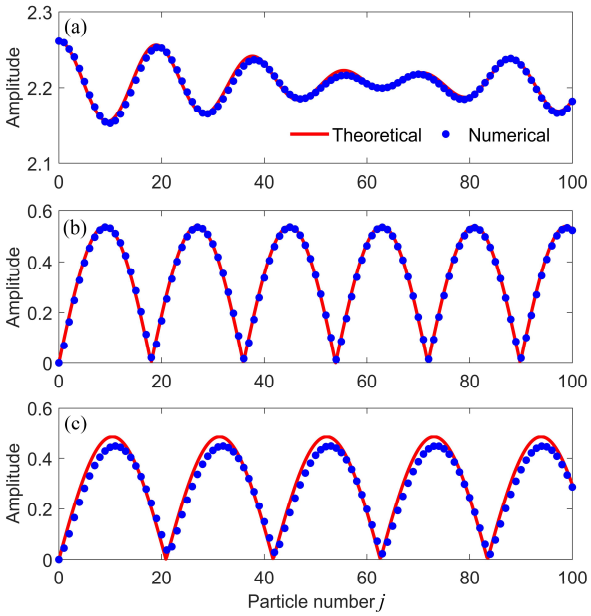

FIG. 3. (Color online) Amplitude profiles of different frequency components of the rotational wave along the nonlinear monoatomic granular chain with no substrate. (a) Fundamental frequency (FF) wave with $\omega_{TR} = 2.3$; (b) sum-frequency (SF) component; (c) difference-frequency (DF) component.

B. Nonlinear wave dynamics in a granular chain on a substrate

Now we consider the chain-substrate system where only the linear normal coupling exists, e.g., $g_n = 2$, $g_s = 0$. To ensure the FF waves and the generated frequency components are located in different TR modes, a higher frequency of the longitudinal FF wave is chosen in this section, i.e., $\omega_L = 1.5$. Under these conditions, the nonlinear dispersion curves of the TR waves are plotted in Fig. 4.

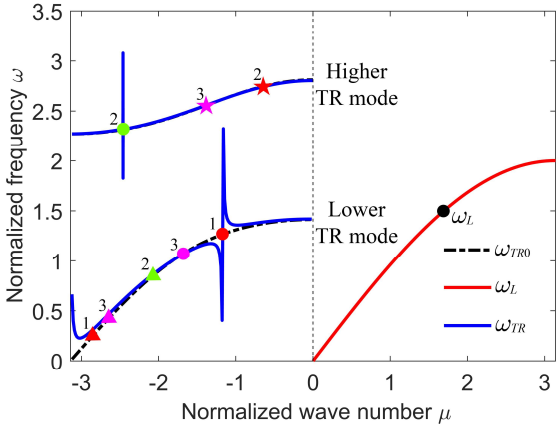

FIG. 4. (Color online) Nonlinear dispersion relations (red solid lines for longitudinal wave, blue solid lines for the TR waves) with nonlinear resonances of the granular chain on a substrate. The black dashed lines are the linear dispersion relations. Circle markers: fundamental frequency (FF) waves; star markers: sum-frequency (SF) components; triangle markers: difference-frequency (DF) components. No. 1: nonlinear resonance between FF and SF components; No. 2: nonlinear resonance between FF and DF components; No. 3: no resonance.

It is seen that two resonances appear at critical wave number values in the nonlinear dispersion curves. The one belonging to the lower TR mode is the resonance between FF and SF components, which satisfies the condition (37a), as listed in Table II and illustrated by the markers 1 in Fig. 4. The other one belonging to the higher TR mode is the resonance between FF and DF components, which satisfies the condition (37b), as listed in Table III and illustrated by the markers 2 in Fig. 4.

TABLE II. Parameters of the wave components at the lower nonlinear resonance

Component	Longitudinal FF wave	TR FF wave	TR SF component	TR DF component
Frequency	$\omega_L = 1.5$	$\omega_{TR}^- = 1.265$	$\omega_{TR}^- + \omega_L = 2.765$	$\omega_L - \omega_{TR}^- = 0.235$
Wave number	$\mu(\omega_L) = 1.696$	$\mu(\omega_{TR}^-) = -1.175$	$\mu(\omega_{TR}^- + \omega_L) = -0.519$	$\mu(\omega_L - \omega_{TR}^-) = -2.871$
Location	Longitudinal mode	Lower TR mode	Higher TR mode	Lower TR mode

TABLE III. Parameters of the wave components at the higher nonlinear resonance

Component	Longitudinal FF wave	TR FF wave	TR SF component	TR DF component
Frequency	$\omega_L = 1.5$	$\omega_{TR}^+ = 2.315$	$\omega_{TR}^+ + \omega_L = 3.815$	$\omega_{TR}^+ - \omega_L = 0.815$
Wave number	$\mu(\omega_L) = 1.696$	$\mu(\omega_{TR}^+) = -2.459$	– –	$\mu(\omega_{TR}^+ - \omega_L) = -2.128$

Location	Longitudinal mode	Higher TR mode	Band gap	Lower TR mode

TABLE IV. Parameters of the wave components in the case of no resonance

Component	Longitudinal FF wave	TR FF wave	TR SF component	TR DF component
Frequency	$\omega_L = 1.5$	$\omega_{TR}^- = 1.1$	$\omega_{TR}^- + \omega_L = 2.6$	$\omega_L - \omega_{TR}^- = 0.4$
Wave number	$\mu(\omega_L) = 1.696$	$\mu(\omega_{TR}^-) = -1.622$	$\mu(\omega_{TR}^- + \omega_L) = -1.235$	$\mu(\omega_L - \omega_{TR}^-) = -2.675$
Location	Longitudinal mode	Lower TR mode	Higher TR mode	Lower TR mode

The peak at the Brillouin zone edge $\mu = -\pi$ is caused by the zero-frequency TR mode acting as the divisor in Eqs. (28). We do not explore it here. It is necessary to stress that the resonance peaks shown in the dispersion curves do not indicate infinite values of frequency, since around the resonances, the MTSM used to derive dispersion relations is invalid when the frequency correctors are large. Therefore, these frequency values at the resonances are approximately calculated by the linear dispersion relations. Nevertheless, these peaks accurately provide the wave number values at the resonances, as they are caused mathematically by the singularities in the formulation.

To compare with the wave dynamics at the nonlinear resonance, we first address the no resonance case, as illustrated by the markers 3 in Fig. 4. The parameters are listed in Table IV. It is shown in Fig. 5 that in this case the amplitudes of the different frequency components behave similarly to those in the monoatomic granular chain without substrate (see Fig. 3). The beating periods of the SF and DF components are $j_{SF} = 2\pi / \left|\Delta\mu_{TR}^+\right| \approx 5$ and $j_{DF} = 2\pi / \left|\Delta\mu_{TR}^-\right| \approx 20$. The theoretical results agree well with the numerical simulations for the SF and DF components. The observed discrepancy for the FF wave could be explained by considering that a small portion of its energy is transferred to the frequency components other than SF and DF. In this case, an inter-mode energy transfer can be observed due to the frequency hopping of the SF component from the lower TR mode to the higher one.

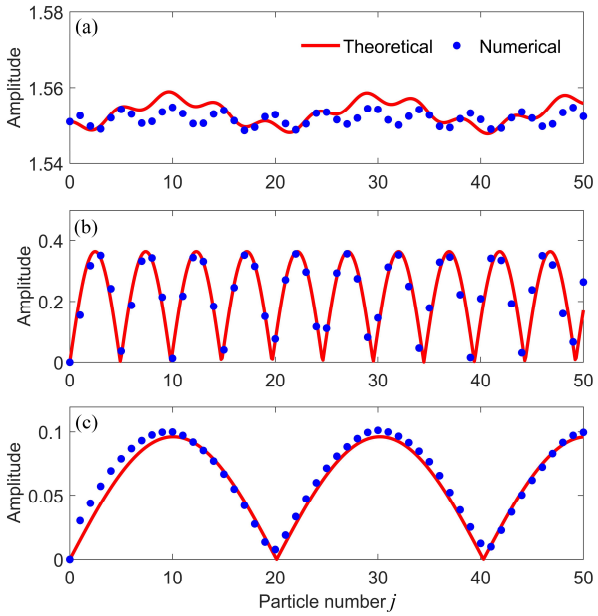

FIG. 5. (Color online) Amplitude profiles of different frequency components of the rotational wave in the no resonance case in the nonlinear chain-substrate system. (a) Fundamental frequency (FF) wave with $\omega_{TR}^- = 1.1$; (b) sum-frequency (SF) component; (c) difference-frequency (DF) component.

As the nonlinear resonances take place, the regular MTSM is no longer valid and fails to predict the physical behaviour due to singularity appearance [**28**]. In such a case, an analytical solution appears, at present, to be out of reach. Hence, the problem is solved numerically instead.

The numerical results (blue dots) for different frequency component amplitudes in the case of nonlinear resonance between FF and SF components (see Table II and the markers 1 in Fig. 4) are given in Figs. 6 and 7. To better illustrate the profiles of the oscillations, the numerical results are curve-fitted as shown by the black dashed lines. The resonance is characterized by a highly efficient energy transfer from the FF waves to the SF components. In particular, the FF wave amplitudes are reduced to near zero values along the chain, whereas the SF component

amplitudes initially oscillate to then stabilise at some constant values. These processes are accompanied by the oscillations in the wave component amplitudes due to the wave numbers asynchronism described by Eqs. (37).

The period of the SF component amplitude oscillations is $j_{SF} \approx 6$, and that of the DF component amplitudes is $j_{DF} \approx 12$. The FF wave amplitudes are predicted to oscillate with a period that is the lowest common multiple of j_{SF} and j_{DF}, provided that the magnitudes of the SF and DF components are of the same order, as given by Eqs. (31). However, note that under the resonance, the magnitudes of the DF components are much smaller than those of the SF components, and therefore they have a weak influence on the oscillation period of the FF wave amplitudes. This leads to the FF wave amplitudes to approximately oscillate with the same period as that of the SF components.

From these results, it can be concluded that for a long enough chain the energy could be transferred completely from the FF waves to the generated wave components, especially to the SF components under this resonance. However, in practice, the complete energy transfer could be limited by the presence of dissipation.

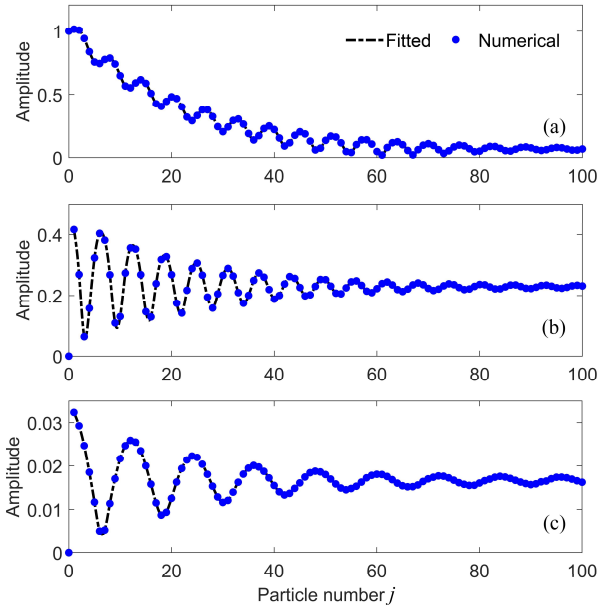

FIG. 6. (Color online) Amplitude profiles of different frequency components of the transverse waves at the lower nonlinear resonance in the nonlinear chain-substrate system. (a) Fundamental frequency (FF) wave with $\omega_{TR}^{-} = 1.265$; (b) sum-frequency (SF) component; (c) difference-frequency (DF) component.

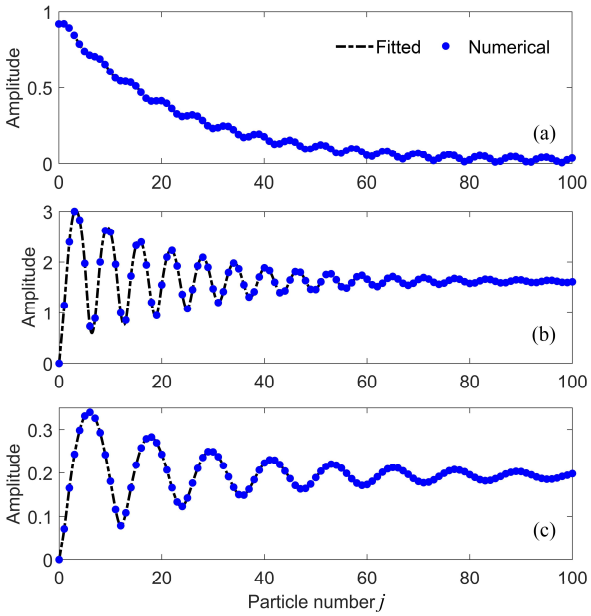

FIG. 7. (Color online) Amplitude profiles of different frequency components of the rotational waves at the lower nonlinear resonance in the nonlinear chain-substrate system. (a) Fundamental frequency (FF) wave with $\omega_{TR}^{-} = 1.265$; (b) sum-frequency (SF) component; (c) difference-frequency (DF) component.

The time domain waveforms and the corresponding power spectral densities (PSDs) of the rotational waves are shown in Fig. 8, as obtained from the simulations for the j=1 and j=100 particles. Here the PSD is calculated as the magnitude squared of the signal's Fourier transform under unit frequency width. One can observe that the PSD magnitude of the FF component at the j=100 particle is reduced to a small value, while that of the SF component becomes approximately twice that of the first j=1 particle. This also confirms the highly efficient energy transfer due to the nonlinear resonance.

In addition, it is worth mentioning that the energy transfer under the conditions of the nonlinear resonance discussed above is irreversible. This means that, when the wave with the frequency $\omega_{TR}^{-} + \omega_L$ is excited in the system and the DF components with the frequency ω_{TR}^{-} are generated as it propagates through the chain, the resonance will not be achieved as the resonance conditions (37) are not satisfied.

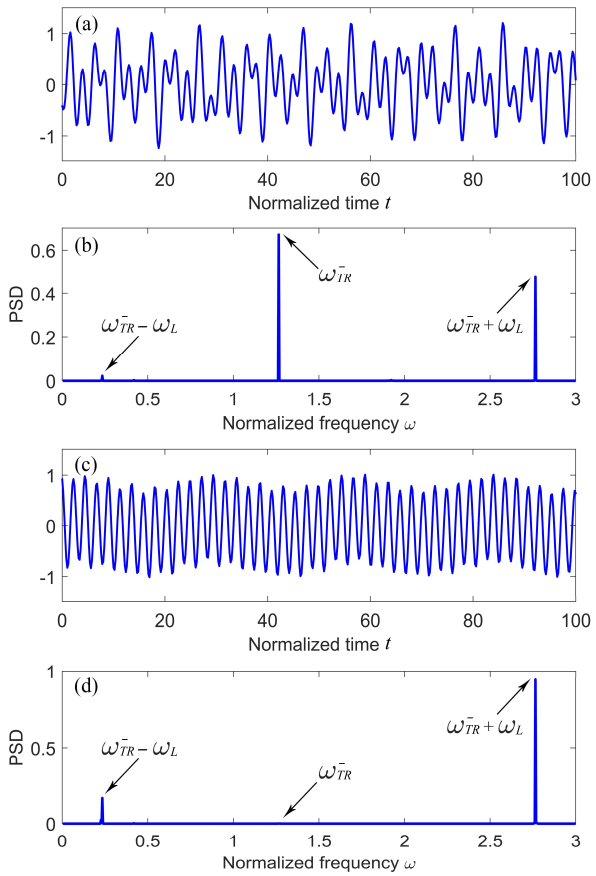

FIG. 8. (Color online) Time domain waveforms and power spectral densities (PSDs) of (a)-(b) j=1 particle and (c)-(d) j=100 particle under the nonlinear resonance. The fundamental frequency of the TR waves is $\omega_{TR}^{-}=1.265$.

On the other hand, when the FF waves are injected from the nonlinear resonance on the higher TR mode, the DF components are generated on the lower TR mode and the SF components fall into the band gap (see Table III and the markers 2 in Fig. 4).

The amplitudes of different frequency components shown in Figs. 9 and 10 exhibit similar spatial profiles as those for the former resonance. However, the injected energy of the FF waves pumps mostly to the DF components under this resonance. The black dashed lines in the figures are plotted by curve-fitting the numerical results to better show profiles of the oscillation. The oscillations of these wave components are not clearly distinguished since their period is small, i.e., $j_{DF}\approx 3$. In particular, the amplitude in Fig. 9(a) shows minuscule oscillation. This could be because the DF component has small oscillation magnitudes [see Fig. 9(b)] and its influence on FF wave amplitudes is not significant. The amplitudes of the SF components shown in Fig. 9(c) and 10(c) are exponentially damped to small values within the band gap and, therefore, it is reasonable to expect that these have negligible influence on the system dynamics.

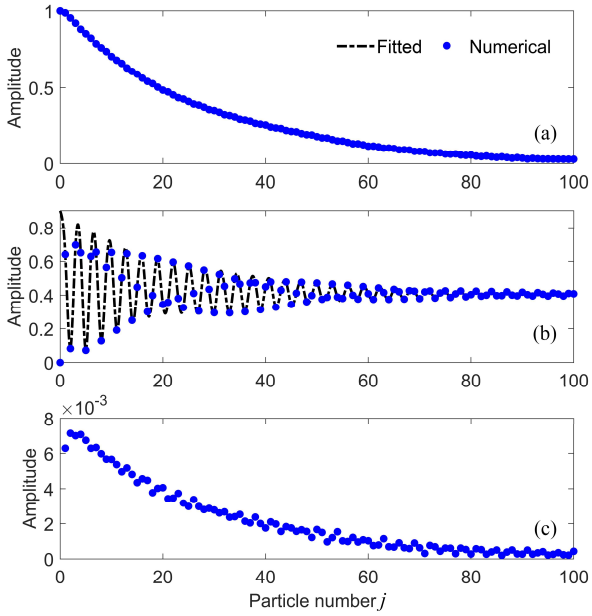

FIG. 9. (Color online) Amplitude profiles of different frequency components of the transverse waves at the higher nonlinear resonance in the nonlinear chain-substrate system. (a) Fundamental frequency (FF) wave with $\omega_{TR}^{+}=2.315$; (b) sum-frequency (SF) component; (c) difference-frequency (DF) component.

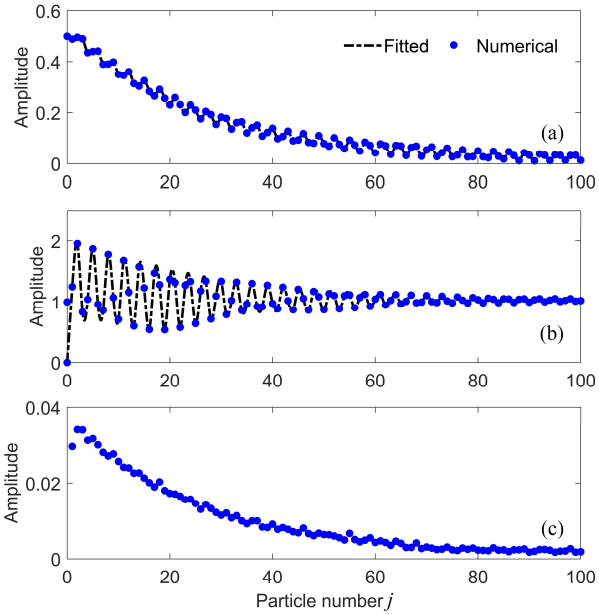

FIG. 10. (Color online) Amplitude profiles of different frequency components of the rotational waves at the higher

nonlinear resonance in the nonlinear chain-substrate system. (a) Fundamental frequency (FF) wave with $\omega_{TR}^{+}=2.315$; (b) sum-frequency (SF) component; (c) difference-frequency (DF) component.

V. CONCLUSIONS

This work investigated the nonlinear coupled wave dynamics in one-dimensional granular chains, with and without a substrate, by taking into account the nonlinear interactions between the longitudinal and the transverse-rotational waves. The nonlinear interactions lead to the generations of the sum-frequency and the difference-frequency components of the transverse-rotational waves, as the fundamental frequency waves propagate along the chain. By means of the multiple time scale method, we calculated the analytical solutions for these wave components in the semi-infinite chains, as well as the nonlinear dispersion curves for the infinite systems.

It was shown that in a monoatomic granular chain without substrate, the nonlinear dispersion curves of the coupled waves are slightly modified by the weak nonlinearity of the system and the amplitudes of different wave components are characterized by the spatial beating oscillations whose periods are determined by the wave number mismatch due to the wave dispersion.

For a granular chain coupled to a substrate, the system exhibits nonlinear resonances with time-space asynchronism conditions, which have been predicted analytically and correspond to one of the key contributions of this work. At these resonances, the fundamental frequency wave amplitudes decrease and the generated frequency component amplitudes increase in the process of propagation, being accompanied by the occurrence of oscillations which result from the wave numbers asynchronism. It is hence concluded that for a long enough chain the energy could be transferred completely from the fundamental frequency waves to the generated frequency components.

The results of this work provide a theoretical basis for understanding the nonlinear coupled wave process in granular crystals with and without a substrate, accounting for the transverse and rotational degrees of freedom. It is envisaged that the results of this paper could inspire the design of acoustic devices for irreversible energy transfer, energy harvesting, and energy rectification.

ACKNOWLEDGEMENTS

Qicheng Zhang thanks China Scholarship Council and Harbin Engineering University, China for providing an International Scholarship (No. 201806680075) that has supported his work at the University of Salford, UK.

APPENDIX

A

This appendix provides the pre-factors a_1, b_1, c_1, d_1 and e_1 of the Φ functions [see Eqs. (22)] that allow solving the first order EOMs. These are

$$a_1 = 2ik_2\left(2\sin\left[\mu(\omega_{L0})\right]-\sin\left[2\mu(\omega_{L0})\right]\right)\cdot\left|A_0\right|^2,$$

$$\begin{aligned} b_1 &= 2is_2\left(\sin\left[\mu(\omega_{L0})\right]+\sin\left[\mu(\omega_{TR0})\right]-\sin\left[\mu(\omega_{TR0})+\mu(\omega_{L0})\right]\right)\cdot\left|A_0\right|\left|B_0\right| \\ &\quad -2s_2\left(1-\cos\left[\mu(\omega_{L0})\right]+\cos\left[\mu(\omega_{TR0})\right]-\cos\left[\mu(\omega_{TR0})+\mu(\omega_{L0})\right]\right)\cdot\left|A_0\right|\left|C_0\right|, \end{aligned}$$

$$\begin{aligned} c_1 &= -2r_2\left(1-\cos\left[\mu(\omega_{L0})\right]-\cos\left[\mu(\omega_{TR0})\right]+\cos\left[\mu(\omega_{TR0})+\mu(\omega_{L0})\right]\right)\cdot\left|A_0\right|\left|B_0\right| \\ &\quad +2ir_2\left(\sin\left[\mu(\omega_{L0})\right]-\sin\left[\mu(\omega_{TR0})\right]+\sin\left[\mu(\omega_{TR0})+\mu(\omega_{L0})\right]\right)\cdot\left|A_0\right|\left|C_0\right|, \end{aligned}$$

$$\begin{aligned} d_1 &= 2is_2\left(-\sin\left[\mu(\omega_{L0})\right]+\sin\left[\mu(\omega_{TR0})\right]-\sin\left[\mu(\omega_{TR0})-\mu(\omega_{L0})\right]\right)\cdot\left|\bar{A}_0\right|\left|B_0\right| \\ &\quad -2s_2\left(1-\cos\left[\mu(\omega_{L0})\right]+\cos\left[\mu(\omega_{TR0})\right]-\cos\left[\mu(\omega_{TR0})-\mu(\omega_{L0})\right]\right)\cdot\left|\bar{A}_0\right|\left|C_0\right|, \end{aligned}$$

$$\begin{aligned} e_1 &= -2r_2\left(1-\cos\left[\mu(\omega_{L0})\right]-\cos\left[\mu(\omega_{TR0})\right]+\cos\left[\mu(\omega_{TR0})-\mu(\omega_{L0})\right]\right)\cdot\left|\bar{A}_0\right|\left|B_0\right| \\ &\quad -2ir_2\left(\sin\left[\mu(\omega_{L0})\right]+\sin\left[\mu(\omega_{TR0})\right]-\sin\left[\mu(\omega_{TR0})-\mu(\omega_{L0})\right]\right)\cdot\left|\bar{A}_0\right|\left|C_0\right|. \end{aligned} \tag{A1}$$

B

This appendix details the resolution process of the second order EOMs (27) where the frequency correctors and wave solutions are calculated at the said order. By substituting the zeroth and first order solutions [Eqs. (14) and (20)] into Eqs. (27), and recalling that these are independent of τ_1, the equations are simplified to

$$\begin{aligned}&\frac{\partial^2 u_j^{(2)}}{\partial \tau_0^2}+k_1\left(2u_j^{(2)}-u_{j-1}^{(2)}-u_{j+1}^{(2)}\right)\\&=f_1 e^{i\alpha_{jL}}+g_1 e^{i\left(2\beta_{jL}-\alpha_{jL}\right)}+OFCs+c.c.,\end{aligned}$$

$$\begin{aligned}&\frac{\partial^2 w_j^{(2)}}{\partial \tau_0^2}+s_1\left(2w_j^{(2)}-w_{j-1}^{(2)}-w_{j+1}^{(2)}\right)+s_1\left(\varphi_{j+1}^{(2)}-\varphi_{j-1}^{(2)}\right)\\&=h_1 e^{i\alpha_{jTR}}+m_1 e^{i\left(\beta_{jTR}+\beta_{jL}-\alpha_{jL}\right)}+n_1 e^{i\left(\beta_{jTR}-\beta_{jL}+\alpha_{jL}\right)}+OFCs+c.c.,\\&\frac{\partial^2 \varphi_j^{(2)}}{\partial \tau_0^2}+r_1\left(2\varphi_j^{(2)}+\varphi_{j-1}^{(2)}+\varphi_{j+1}^{(2)}\right)+r_1\left(w_{j-1}^{(2)}-w_{j+1}^{(2)}\right)\\&=o_1 e^{i\alpha_{jTR}}+p_1 e^{i\left(\beta_{jTR}+\beta_{jL}-\alpha_{jL}\right)}+q_1 e^{i\left(\beta_{jTR}-\beta_{jL}+\alpha_{jL}\right)}+OFCs+c.c..\end{aligned}\tag{B1}$$

On the right-hand sides of Eqs. (B1), the terms with $e^{i\alpha_{jL}}$ and $e^{i\alpha_{jTR}}$ are secular terms that are eliminated, whereas the terms with $e^{i\left(2\beta_{jL}-\alpha_{jL}\right)}$, $e^{i\left(\beta_{jTR}+\beta_{jL}-\alpha_{jL}\right)}$ and $e^{i\left(\beta_{jTR}-\beta_{jL}+\alpha_{jL}\right)}$ are the contributors to the fundamental waves caused by the nonlinear wave interactions. The acronym *OFCs* stands for "other frequency components" resulting from the combinations of different frequency components.

The pre-factors of the secular terms in Eqs. (B1) are

$$f_1=2i\omega_{L0}\frac{\partial A_0}{\partial \tau_2}-4ik_2\left(2\sin\left[\mu(\omega_{L0})\right]-\sin\left[2\mu(\omega_{L0})\right]\right)\cdot\left|\bar{A}_0\right|A_{1P},$$

$$\begin{aligned}h_1=&\,2i\omega_{TR0}\frac{\partial B_0}{\partial \tau_2}-2is_2\left(\sin\left[\mu(\omega_{L0})\right]+\sin\left[\mu(\omega_{TR0})\right]-\sin\left[\mu(\omega_{TR0})+\mu(\omega_{L0})\right]\right)\cdot\left|\bar{A}_0\right|B_{1P}\\&-2s_2\left(1-\cos\left[\mu(\omega_{L0})\right]-\cos\left[\mu(\omega_{TR0})\right]+\cos\left[\mu(\omega_{TR0})+\mu(\omega_{L0})\right]\right)\cdot\left|\bar{A}_0\right|C_{1P}\\&+2is_2\left(\sin\left[\mu(\omega_{L0})\right]-\sin\left[\mu(\omega_{TR0})\right]+\sin\left[\mu(\omega_{TR0})-\mu(\omega_{L0})\right]\right)\cdot\left|A_0\right|D_{1P}\\&-2s_2\left(1-\cos\left[\mu(\omega_{L0})\right]-\cos\left[\mu(\omega_{TR0})\right]+\cos\left[\mu(\omega_{TR0})-\mu(\omega_{L0})\right]\right)\cdot\left|A_0\right|E_{1P},\end{aligned}$$

$$\begin{aligned}o_1=&\,2i\omega_{TR0}\frac{\partial C_0}{\partial \tau_2}-2r_2\left(1-\cos\left[\mu(\omega_{L0})\right]+\cos\left[\mu(\omega_{TR0})\right]-\cos\left[\mu(\omega_{TR0})+\mu(\omega_{L0})\right]\right)\cdot\left|\bar{A}_0\right|B_{1P}\\&-2ir_2\left(\sin\left[\mu(\omega_{L0})\right]-\sin\left[\mu(\omega_{TR0})\right]+\sin\left[\mu(\omega_{TR0})+\mu(\omega_{L0})\right]\right)\cdot\left|\bar{A}_0\right|C_{1P}\\&-2r_2\left(1-\cos\left[\mu(\omega_{L0})\right]+\cos\left[\mu(\omega_{TR0})\right]-\cos\left[\mu(\omega_{TR0})-\mu(\omega_{L0})\right]\right)\cdot\left|A_0\right|D_{1P}\\&+2ir_2\left(\sin\left[\mu(\omega_{L0})\right]+\sin\left[\mu(\omega_{TR0})\right]-\sin\left[\mu(\omega_{TR0})-\mu(\omega_{L0})\right]\right)\cdot\left|A_0\right|E_{1P}.\end{aligned}\tag{B2}$$

By setting these pre-factors to zero, the second order frequency correctors to the linear dispersion relations, presented in Eqs. (28), can be obtained.

In addition, the pre-factors of the fundamental wave contributors in Eqs. (B1) are

$$g_1=-4ik_2\left(\sin\left[\mu(\omega_{L0})\right]+\sin\left[\mu(2\omega_{L0})-\mu(\omega_{L0})\right]-\sin\left[\mu(2\omega_{L0})\right]\right)\cdot\left|\bar{A}_0\right|A_{1H},$$

$$\begin{aligned}m_1=&-2is_2\left(\sin\left[\mu(\omega_{L0})\right]+\sin\left[\mu(\omega_{TR0}+\omega_{L0})-\mu(\omega_{L0})\right]-\sin\left[\mu(\omega_{TR0}+\omega_{L0})\right]\right)\cdot\left|\bar{A}_0\right|B_{1H}\\&-2s_2\left(1-\cos\left[\mu(\omega_{L0})\right]-\cos\left[\mu(\omega_{TR0}+\omega_{L0})-\mu(\omega_{L0})\right]+\cos\left[\mu(\omega_{TR0}+\omega_{L0})\right]\right)\cdot\left|\bar{A}_0\right|C_{1H},\end{aligned}$$

$$\begin{aligned}n_1=&\,2is_2\left(\sin\left[\mu(\omega_{L0})\right]-\sin\left[\mu(\omega_{TR0}-\omega_{L0})+\mu(\omega_{L0})\right]+\sin\left[\mu(\omega_{TR0}-\omega_{L0})\right]\right)\cdot\left|A_0\right|D_{1H}\\&-2s_2\left(1-\cos\left[\mu(\omega_{L0})\right]-\cos\left[\mu(\omega_{TR0}-\omega_{L0})+\mu(\omega_{L0})\right]+\cos\left[\mu(\omega_{TR0}-\omega_{L0})\right]\right)\cdot\left|A_0\right|E_{1H},\end{aligned}$$

$$p_1 = -2r_2\left(1-\cos\left[\mu(\omega_{L0})\right]+\cos\left[\mu(\omega_{TR0}+\omega_{L0})-\mu(\omega_{L0})\right]-\cos\left[\mu(\omega_{TR0}+\omega_{L0})\right]\right)\cdot\left|\bar{A}_0\right|B_{1H}$$
$$-2ir_2\left(\sin\left[\mu(\omega_{L0})\right]-\sin\left[\mu(\omega_{TR0}+\omega_{L0})-\mu(\omega_{L0})\right]+\sin\left[\mu(\omega_{TR0}+\omega_{L0})\right]\right)\cdot\left|\bar{A}_0\right|C_{1H},$$

$$q_1 = -2r_2\left(1-\cos\left[\mu(\omega_{L0})\right]+\cos\left[\mu(\omega_{TR0}-\omega_{L0})+\mu(\omega_{L0})\right]-\cos\left[\mu(\omega_{TR0}-\omega_{L0})\right]\right)\cdot\left|A_0\right|D_{1H}$$
$$+2ir_2\left(\sin\left[\mu(\omega_{L0})\right]+\sin\left[\mu(\omega_{TR0}-\omega_{L0})+\mu(\omega_{L0})\right]-\sin\left[\mu(\omega_{TR0}-\omega_{L0})\right]\right)\cdot\left|A_0\right|E_{1H}. \quad \text{(B3)}$$

According to the right-hand sides of the second order EOMs (B1), the particular solutions of the second order solutions are assumed to be

$$u_{j,P}^{(2)} = A_{2P}e^{i\left(2\beta_{jL}-\alpha_{jL}\right)}+c.c.,$$

$$w_{j,P}^{(2)} = B_{2P}e^{i\left(\beta_{jTR}+\beta_{jL}-\alpha_{jL}\right)}+D_{2P}e^{i\left(\beta_{jTR}-\beta_{jL}+\alpha_{jL}\right)}+c.c.,$$

$$\varphi_{j,P}^{(2)} = C_{2P}e^{i\left(\beta_{jTR}+\beta_{jL}-\alpha_{jL}\right)}+E_{2P}e^{i\left(\beta_{jTR}-\beta_{jL}+\alpha_{jL}\right)}+c.c.. \quad \text{(B4)}$$

By substituting these solutions into the second order EOMs (B1) and equating the coefficients, one obtains

$$A_{2P} = g_1\cdot\Phi_0\left(\omega_{L0},\mu(2\omega_{L0})-\mu(\omega_{L0})\right),$$

$$B_{2P} = m_1\cdot\Phi_1\left(\omega_{TR0},\mu(\omega_{TR0}+\omega_{L0})-\mu(\omega_{L0})\right)$$
$$+p_1\cdot\Phi_2\left(\omega_{TR0},\mu(\omega_{TR0}+\omega_{L0})-\mu(\omega_{L0})\right),$$

$$D_{2P} = n_1\cdot\Phi_1\left(\omega_{TR0},\mu(\omega_{TR0}-\omega_{L0})+\mu(\omega_{L0})\right)$$
$$+q_1\cdot\Phi_2\left(\omega_{TR0},\mu(\omega_{TR0}-\omega_{L0})+\mu(\omega_{L0})\right),$$

$$C_{2P} = m_1\cdot\Phi_3\left(\omega_{TR0},\mu(\omega_{TR0}+\omega_{L0})-\mu(\omega_{L0})\right)$$
$$+p_1\cdot\Phi_4\left(\omega_{TR0},\mu(\omega_{TR0}+\omega_{L0})-\mu(\omega_{L0})\right),$$

$$E_{2P} = n_1\cdot\Phi_3\left(\omega_{TR0},\mu(\omega_{TR0}-\omega_{L0})+\mu(\omega_{L0})\right)$$
$$+q_1\cdot\Phi_4\left(\omega_{TR0},\mu(\omega_{TR0}-\omega_{L0})+\mu(\omega_{L0})\right). \quad \text{(B5)}$$

Subsequently, the general solutions of the homogeneous equations take the following forms that contain the terms of fundamental frequencies

$$u_{j,H}^{(2)} = A_{2H}e^{i\alpha_{jL}}+c.c.,$$

$$w_{j,H}^{(2)} = B_{2H}e^{i\alpha_{jTR}}+c.c.,$$

$$\varphi_{j,H}^{(2)} = C_{2H}e^{i\alpha_{jTR}}+c.c.. \quad \text{(B6)}$$

The coefficients here are also determined by the boundary conditions described previously [$u_0^{(2)}\left(2\omega_{L0}\right)=0$, $w_0^{(2)}\left(\omega_{TR0}\pm\omega_{L0}\right)=0$ and $\varphi_0^{(2)}\left(\omega_{TR0}\pm\omega_{L0}\right)=0$] as

$$A_{2H} = -A_{2P},$$

$$B_{2H} = -\left(B_{2P}+D_{2P}\right),$$

$$C_{2H} = -\left(C_{2P}+E_{2P}\right). \quad \text{(B7)}$$

Under these conditions, the second order solutions (20), which contain only the contributions of the FF waves, are simplified into Eqs. (29).

[**1**] K. L. Johnson, *Contact Mechanics* (Cambridge University Press, Cambridge, 1985).
[**2**] V. F. Nesterenko, *Dynamics of Heterogeneous Materials* (Spring-Verlag, New York, 2001).
[**3**] E. B. Herbold, J. Kim, V. F. Nesterenko, S. Y. Wang, and C. Daraio, Acta Mech. 205, **85** (2009).
[**4**] N. Boechler, J. Yang, G. Theocharis, P. G. Kevrekidis, and C. Daraio, J. Appl. Phys. **109**, 074906 (2011).
[**5**] J. Hong, Phys. Rev. Lett. **94**, 108001 (2005).
[**6**] F. Fraternali, M. A. Porter, and C. Daraio, Mech. Adv. Mater. Struc. **17**, 1 (2010).
[**7**] A. Spadoni and C. Daraio, Proc. Natl. Acad. Sci. **107**, 7230 (2010).
[**8**] F. Allein, V. Tournat, V. E. Gusev, and G. Theocharis, Appl. Phys. Lett. **108**, 161903 (2016).
[**9**] H. Pichard, A. Duclos, J. -P. Groby, V. Tournat, and V. E. Gusev, Phys. Rev. E **89**, 013201 (2014).
[**10**] F. Allein, V. Tournat, V. E. Gusev, and G. Theocharis, Extreme, Mech. Lett. **12**, 65 (2017).
[**11**] Q. Zhang, R. Venegas, O. Umnova, and Y. Lan, Wave Motion **90**, 51 (2019).
[**12**] N. Boechler, G. Theocharis, and C. Daraio, Nat. Mater. **10**, 665 (2011).
[**13**] J. Lydon, G. Theocharis, and C. Daraio, Phys. Rev. E **91**, 023208 (2015).
[**14**] K. Li and P. Rizzo, J. Appl. Phys. **117**, 215101 (2015).
[**15**] C. Chong, E. Kim, E. G. Charalampidis, H. Kim, F. Li, P. G. Kevrekidis, J. Lydon, C. Daraio, and J. Yang, Phys. Rev. E **93**, 052203 (2016).
[**16**] M. A. Hasan, Y. Starosvetsky, A. F. Vakakis, and L. I. Manevitch, Physica D **252**, 46 (2013).
[**17**] V. J. Sanchez-Morcillo, I. Perez-Arijona, and V. Romero-Garcia, Phys. Rev. E **88**, 043203 (2013).
[**18**] J. Cabaret, V. Tournat, and P. Bequin, Phys. Rev. E **86**, 041305 (2012).

[**19**] B. Dubus, N. Swinteck, K. Muralidharan, J. O. Vasseur, and P. A. Deymier, J. Vib. Acoust. **138**, 041016 (2016).
[**20**] R. Ganesh and S. Gonella, Phys. Rev. Lett. **114**, 054302 (2015).
[**21**] P. S. Landa, *Nonlinear Oscillators and Waves in Dynamics Systems* (Springer Science+Business Media, Dordrecht, 1996).
[**22**] A. F. Vakakis, O. V. Gendelman, L. A. Bergman, D. M. McFarland, G. Kerschen, and Y. S. Lee, *Nonlinear Targeted Energy Transfer in Mechanical and Structural Systems* (Springer-Verlag, Berlin and New York, 2008).
[**23**] Y. Starosvetsky, M. A. Hasan, A. F. Vakakis, and L. I. Manevitch, SIAM J. Appl. Math. **72**, 337 (2012).
[**24**] Y. Zhang, K. J. Moore, D. M. McFarland, and A. F. Vakakis, J. Appl. Phys. **118**, 234901 (2015).
[**25**] A. F. Vakakis, L. I. Manevitch, O. V. Gendelman, and L. A. Bergman, J. Sound Vib. **264**, 559 (2003).
[**26**] S. P. Wallen and N. Boechler, Wave Motion **68**, 22 (2017).
[**27**] I. C. Khoo and Y. K. Wang, J. Math. Phys. **17**, 222 (1976).
[**28**] J. Kevorkian and J. D. Cole, *Multiple Scale and Singular Perturbation Methods* (Springer-Verlag, New York, 1996).
[**29**] K. Manktelow, M. J. Leamy, and M. Ruzzene, Nonlinear Dyn. **63**, 193 (2011).
[**30**] R. K. Narisetti, M. J. Leamy, and M. Ruzzene, J. Vib. Acoust. **132**, 031001 (2010).
[**31**] L. Zheng, V. Tournat, and V. E. Gusev, Extreme Mech. Lett. **12**, 55 (2017).
[**32**] MATLAB and Statistics Toolbox Release 2017b, The MathWorks, Inc., Natick, Massachusetts, United States.
[**33**] A. S. Gorshkov, O. N. Ermakova, and V. F. Marchenko, Nonlinearity **10**, 1007 (1997).